PERGAMON

International Journal of Heat and Mass Transfer 44 (2001) 215–233

International Journal of HEAT and MASS TRANSFER

www.elsevier.com/locate/ijhmt

A method of control of transfer processes

P. Furmanski [1], J.M. Floryan*

Department of Mechanical and Materials Engineering, The University of Western Ontario, London, Ont., Canada N6A 5B9

Received 1 December 1997

Abstract

The effective medium theory for the coupled phenomena of heat conduction and mass diffusion of solute in heterogeneous media has been derived. The theory has been applied to a barrier with adaptive conductive and diffusive characteristics to be used for control of heat flow and mass flow of species. The barrier consists of a mixture of small solid particles of ellipsoidal shape which are randomly distributed in a carrier fluid. Volume fraction of the particles is small and variation in conductive–diffusive properties of the barrier is achieved by changing orientation of the particles. This analysis gives an estimate to what a degree the solute flow can be controlled by both bulk concentration and temperature gradient applied to the walls of the barrier. Influence of different parameters like ratios of conductive and diffusive properties of particles and the carrier fluid, solubility ratio of the diffusing species in the fluid and in the particle, class of particle shapes, particle aspect ratio and volume fraction as well as thickness of the barrier on the species mass flow have been studied in detail. © 2000 Elsevier Science Ltd. All rights reserved.

1. Introduction

In the past few years different devices were proposed for a control of different modes (conduction, convection, radiation) of heat and mass transfer through "smart walls". They were generally based on an idea of dynamical tuning of corresponding properties of these walls [1–5].

One possible way of the tuning can be achieved by varying internal pressure of a gas, like hydrogen, which, due to its high thermal conductivity, can substantially change the effective conductance of the porous medium filling the wall. This idea had found application in thermal insulations proposed for building design [5]. It was verified experimentally for glass-fiber filled super insulation panels and allowed the panels to adjust heat gains (or heat losses) to the actual environmental conditions (ambient temperature and insolation). Switching between low and high hydrogen pressure in the insulation was achieved by electrical heating or cooling of a metal hydride container. The change of temperature of the container caused a release or absorption of the hydrogen.

The other way of varying properties of the wall is the use of electro- or magneto-rheological fluids. Such fluids are formed by suspensions of highly, electrically or magnetically, polarizable, micron-sized, almost spherical particles distributed in suitable carrier fluids. In the electro-rheological fluids, the electric field of a sufficient strength gives rise to formation of long particle chains (known as electrically induced fibration). When the main mode of heat transfer is radiation, this

* Corresponding author. Tel.: +1-519-661-2130; fax: +1-519-661-3757.

E-mail address: mfloryan@eng.uwo.ca (J.M. Floryan).

[1] Permanent address: Institute of Heat Engineering, Warsaw University of Technology, ul. Nowowiejska 25, 00-665, Warsaw, Poland.

0017-9310/01/$ - see front matter © 2000 Elsevier Science Ltd. All rights reserved.
PII: S0017-9310(00)00073-9

Nomenclature

A	external area of the medium or of the particle
$\boldsymbol{C}_{TT}$, $\boldsymbol{C}_{Tc}$, $\boldsymbol{C}_{cT}$, $\boldsymbol{C}_{cc}$	second order tensors defined in Eq. (38)
c	solute concentration
D_c	generalized solute diffusivity defined in Eq. (3)
$(D_c/M)^*$	complex diffusivity defined in Eqs. (9) and (10)
D_{cf}	solute diffusivity in the fluid
D_{cs}	solute diffusivity in the particles
D_c^{ef*}	effective Soret coefficient determined using only the first term from the expansions of the microstructure functions, defined in Eq. (27)
$D_{c\perp}^{ef}$	component of tensor D_c^{ef*} in the direction normal to the barrier
D_T	generalized Soret coefficient defined in Eq. (3)
D_T^*	complex Soret coefficient defined in Eq. (3)
D_{Tf}	Soret coefficient in the fluid
D_{Ts}	Soret coefficient in the particles
D_T^{ef*}	effective Soret coefficient determined using only the first term from the expansions of the microstructure functions, defined in Eq. (27)
$D_{c\perp}^{ef}$	component of tensor D_T^{ef*} in the direction normal to the barrier
$\boldsymbol{j}$	solute flux
j	solute flux in the direction normal to the barrier
j_f	solute flux in the direction normal to the barrier for the case of pure fluid
L	length of the major (minor) dimension of the rod-like (disk-like) particle
l	microdimension
M	generalized solubility defined in Eq. (3)
m	ratio of solute solubilities in the particle and in the carrier fluid
$\boldsymbol{n}$	external unit vector normal to the surface
R	radius of the spheroidal particle
$\boldsymbol{P}$	particle shape tensor
P	component of the tensor in the direction perpendicular to barrier faces
$\boldsymbol{P}^*$	tensor defined in Eq. (41)
$\boldsymbol{q}$	heat flux
q	heat flux in the direction perpendicular to barrier faces
T	temperature
V	volume of the medium or volume of the particle
v	volume fraction
$\boldsymbol{x}, \boldsymbol{y}$	location vectors
z	coordinate axis perpendicular to barrier faces
Δ	barrier thickness
δ	Dirac's function
λ_T	generalized thermal conductivity defined in Eq. (3)
λ_T^*	complex thermal conductivity defined in Eq. (3)
λ_{Tf}	thermal conductivity of the fluid
λ_{Ts}	thermal conductivity of the particles
λ_T^{ef}	effective thermal conductivity defined in Eq. (24)
λ_T^{ef*}	effective thermal conductivity determined using only the first term from the expansions of the microstructure function, defined in Eq. (27)
$\lambda_{T\perp}^{ef}$	component of tensor λ_T^{ef*} in the direction normal to the barrier
λ_c	generalized Dufour coefficient defined in Eq. (3)
$(\lambda_c/M)^*$	complex Dufour coefficient defined in Eq. (3)
λ_{cf}	Dufour coefficient of the fluid
λ_{cs}	Dufour coefficient of the particles
λ_c^{ef}	effective Dufour coefficient defined in Eq. (24)
λ_c^{ef*}	effective Dufour coefficient determined using only the first term from the expansions of the microstructure function, defined in Eq. (27)
$\lambda_{c\perp}^{ef}$	component of tensor λ_c^{ef*} in the direction normal to the barrier
$\varepsilon(\varepsilon^*)$	aspect ratio of the particle, $\varepsilon = (2R)/L$ for the disk-like particles, $\varepsilon^* = (2R)/L$ for the rod-like particles
κ_T	fluid Dufour coefficient/thermal conductivity ratio
κ_c	fluid Soret coefficient/solute dif-

	fusivity ratio
φ_{TT}	microstructure function associated with temperature field
φ_{Tc}	microstructure function associated with diffusion-thermo effect
φ_{cT}	microstructure function associated with thermo-diffusion effect
φ_{cc}	microstructure function associated with concentration field
σ_{TT}	particle/fluid thermal conductivity ratio
σ_{Tc}	particle/fluid Dufour coefficient ratio
σ_{cT}	particle/fluid Soret coefficient ratio
σ_{cc}	particle/fluid solute diffusivity ratio
θ	characteristic function defined in Eq. (3)
Ω	configuration or pattern of distribution of constituents in the suspension
$\mathbf{1}$	unit second order tensor
∇	Nabla operator
$\{\cdot\}$	ensemble averaging

process of fibration causes the wall to go from an opaque state to a state highly transparent to radiation [2].

In electro- or magneto-rheological suspensions of ferromagnetic powders, thermal conductivity (or mass diffusivity) is increased in the direction of the applied field (electric or magnetic) and reduced in the direction perpendicular to it. Increase of the thermal conductivity (mass diffusivity) and viscosity of the fluids, during their flow, gives rise to an almost three-fold increase in the convective heat (or mass) transfer coefficient [1]. This may cause significant increase in efficiency of heat (or mass) exchangers. Application of a rotating magnetic field produces two kinds of motion in the layer of a ferromagnetic suspension. The first one consists of microscopic intensive vortex motion, due to rotation of the aggregates, and the second one involves macroscopic flow of the entire fluid. This means that the augmentation of heat or mass transfer in the system can be ascribed to the convective transport (macroscopic flow in the suspension) as well as to the pseudoturbulization of the layer by microrotation of the particle aggregates [1].

The third method of changing properties of the "smart wall" is the use of nonspherical particles whose orientation can be controlled. Coating of the particles with a thin layer of either ferromagnetic or ferroelectric material will allow for increase of the torque necessary for rotation of the particles as well as for matching of densities of the particles and the carrier fluid. Upon application of either the electric or magnetic field, orientation of the particles may change. As the particles have properties different than the carrier fluid, the effective conductance of the barrier varies depending on the state of orientation of the particles. The greater the range of variation in the conductance, the higher effectiveness of the barrier. This way of changing properties of the barrier has been previously studied by Furmanski and Floryan [3,4] for the case of heat conduction in the layer of a fluid with suspended rod-like and disk-like particles (in the form of prolate and oblate spheroids). The analysis was carried out for a layer of finite thickness and the relative (particle/fluid) thermal conductivity, particle aspect ratio and their volume fraction were varied. It was found that rotation of the particles by 90° can result in increasing of the heat flux through the barrier by several times. This increase was not sensitive to a small misalignment of the particles. The rod-like particles were more effective when the thermal conductivity of the particles was greater than that of the fluid [3]. The opposite effect was observed for the disk-like particles [4]. They happened to be more effective when their thermal conductivity was smaller than that of the fluid. In both cases of particle shape, the effectiveness of heat flow control was higher due to greater difference in the thermal conductivities of the suspension components. It was also found that an increase in the range of the heat flow control can be achieved by using longer particles and by increasing their volume fraction. The wall effects, associated with the finite thickness of the layer of suspension, tended to decrease the heat flow as compared to the case of an unbounded medium. They were especially pronounced for larger particles and for higher volume fractions of the particles.

The problem of heat and mass flow through a suspension is most conveniently analyzed using the effective medium approach that is popular in the analysis of transfer processes in heterogeneous media ([6–10]. This approach is based upon the replacement of the multicomponent medium by a continuum with either constant or continuously varying effective properties. In the case of the mass flow, such approach was utilized in studies of solute flow in stagnant suspensions under non-reacting and reacting conditions [11,12]. For non-reacting conditions an analogy between the mass diffusion and the thermal conduction is valid in the bulk. This analogy may not be valid on

the boundaries separating different constituents due to the solubility condition that usually leads to a jump in the solute concentration at the particle–fluid interface [13–15]. When convection is present, additional dispersion of the solute may occur due to fluctuations in fluid velocity. This dispersion is included in the effective diffusivity of the medium in the form of velocity dependent terms [16]. For large variation of concentration fields in the medium, these terms may have a nonlocal character [17].

Two averaging techniques are usually applied in order to carry out homogenization leading to the effective medium theory: volume averaging over small physical regions representative of the structure of the medium [18] and ensemble averaging over the ensemble of possible realizations of microgeometry of the medium [10,14].

Phenomena of heat and mass transfer can be mutually coupled (Defourt and Soret effects) [19]. This enables one to control, for example, the mass flow through a "smart wall" using temperature difference applied to the surfaces bounding the wall. Moreover, in the mass transfer problem the fluid and the particles may have different solubilities with respect to the diffusing species. In this paper we are going to address these problems and also study how such cross-effects effect the possible range of control of the solute flow through the layer of suspension. The analysis is based on the effective medium theory using the ensemble averaging technique [20]. The particles are assumed to have random distribution and to constitute a small volume fraction of the mixture (in order to provide enough space for their free rotation). Section 2 discusses adaptation of the effective medium theory to coupled transport phenomena in a heterogeneous medium. In Section 3, the theory is applied to the stationary coupled heat and mass flow through the barrier. Results of parametric study of various factors effecting diffusive mass flow through the barrier for both coupled and uncoupled mass transfer problem are given in Section 4 with a special prominence given to the solubility effects. Finally, Section 6 provides a short summary of the main conclusions.

2. The effective medium theory for coupled transport processes

2.1. Preliminaries

Let us consider coupled phenomena of heat transfer and the transport of a dilute solute through a heterogeneous suspension consisting of a carrier fluid and the particles dispersed in it. In each constituent, the heat transfer and the diffusive mass flow are caused both by the temperature and the concentration gradients

$$\begin{aligned} -\boldsymbol{q} &= \lambda_{\mathrm{T}}\nabla T + (\lambda_{\mathrm{c}}/M)\nabla(Mc), \\ -\boldsymbol{j} &= D_{\mathrm{T}}\nabla T + (D_{\mathrm{c}}/M)\nabla(Mc), \end{aligned} \tag{1}$$

where λ_{T} and D_{c} are respectively, the thermal conductivity and the solute diffusivity, λ_{c} and D_{T} stand for the diffusion-thermo effect coefficient (Dufour coefficient) and the thermo-diffusion effect coefficient (Soret coefficient), respectively, T denotes the temperature, M stands for the solute solubilty, c denotes the solute concentration, and ∇ is the gradient operator.

Heat flux $\boldsymbol{q}$ and mass flux $\boldsymbol{j}$ satisfy steady state conservation equations

$$\nabla\cdot\boldsymbol{q} = 0, \quad \nabla\cdot\boldsymbol{j} = 0 \tag{2}$$

and are functions of the position vector $\boldsymbol{x}$ and the configuration Ω i.e., they are functions of the pattern of distribution of the particles. Ideal thermal contact conditions are assumed at the particle–fluid interface. Equilibrium condition at the particle–fluid interface leads to a step change in the concentration c of the diffusing species. This effect is caused by a different solubility M of the species in the particles and in the fluid. The product of the concentration and the solubility, which we shall refer to as activity, is continuous through the interface. All properties appearing in Eq. (1) are understood to be generalized functions and can be expressed in the following way

$$\begin{aligned} \lambda_{\mathrm{T}}(\boldsymbol{x},\Omega) &= \lambda_{\mathrm{Ts}}\theta(\boldsymbol{x},\Omega) + \lambda_{\mathrm{Tf}}\big[1-\theta(\boldsymbol{x},\Omega)\big], \\ \lambda_{\mathrm{c}}(\boldsymbol{x},\Omega) &= \lambda_{\mathrm{cs}}/m\theta(\boldsymbol{x},\Omega) + \lambda_{\mathrm{cf}}\big[1-\theta(\boldsymbol{x},\Omega)\big], \\ D_{\mathrm{T}}(\boldsymbol{x},\Omega) &= D_{\mathrm{Ts}}\theta(\boldsymbol{x},\Omega) + D_{\mathrm{Tf}}\big[1-\theta(\boldsymbol{x},\Omega)\big], \\ D_{\mathrm{c}}(\boldsymbol{x},\Omega) &= D_{\mathrm{cs}}/m\theta(\boldsymbol{x},\Omega) + D_{\mathrm{cf}}\big[1-\theta(\boldsymbol{x},\Omega)\big], \\ M(\boldsymbol{x},\Omega) &= m\theta(\boldsymbol{x},\Omega) + \big[1-\theta(\boldsymbol{x},\Omega)\big]. \end{aligned} \tag{3}$$

The characteristic function θ is equal to unity for the location inside a particle and is equal to zero inside the fluid. The subscripts s and f correspond to properties of the particles (solid) and the fluid, respectively.

In the effective medium approach, two constituent media are treated as a pseudohomogeneous one with effective properties which account for the properties of the constituents as well as for their distribution in the medium. The notions of temperature and concentration of the diffusing species in this approach should be understood as certain mean quantities averaged either over the representative volume or statistically averaged over an ensemble of possible configurations. The latter way of averaging will be used in the present analysis.

In order to obtain equations describing macroscopic flow of heat and mass in the medium, Eq. (1) and the conservation equations (2) have been ensemble averaged resulting in

$$\nabla \cdot \{\boldsymbol{q}\} = 0, \quad \nabla \cdot \{\boldsymbol{j}\} = 0, \tag{4}$$

$$\begin{aligned} -\{\boldsymbol{q}\} &= \{\lambda_T \nabla T\} + \{(\lambda_c/M)\nabla(Mc)\}, \\ -\{\boldsymbol{j}\} &= \{D_T \nabla T\} + \{(D_c/M)\nabla(Mc)\}. \end{aligned} \tag{5}$$

The above equations have to be supplemented with a "closure scheme" that will allow to express the mean heat flux $\boldsymbol{q}$ and the mean mass flux $\boldsymbol{j}$ by the mean temperature $\{T\}$ and the mean concentration $\{c\}$ of the diffusing species. Eq. (5) can be used to derive the "closure scheme" if the microscopic temperature T and the microscopic concentration c were expressed as functions of the macroscopic fields $\{T\}$ and $\{c\}$.

2.2. Relations between the microscopic and macroscopic (mean) temperature and concentration fields

We begin by substituting Eq. (2) into Eq. (1) and transforming the result into the following form

$$\begin{aligned} &\lambda_{Tf}\nabla^2 T + \lambda_{cf}\nabla^2(Mc) \\ &\quad + \nabla \cdot \left[\lambda_T'\nabla T + (\lambda_c/M)'\nabla(Mc)\right] = 0, \end{aligned} \tag{6}$$

$$\begin{aligned} &D_{Tf}\nabla^2 T + D_{cf}\nabla^2(Mc) \\ &\quad + \nabla \cdot \left[D_T'\nabla T + (D_c/M)'\nabla(Mc)\right] = 0, \end{aligned} \tag{7}$$

where

$$\lambda_T' = \lambda_T - \lambda_{Tf}, \quad (\lambda_c/M)' = \lambda_c/M - \lambda_{Tf},$$

$$D_T' = D_T - D_{Tf}, \quad (D_c/M)' = D_c/M - D_{Tf} \tag{8}$$

Eqs. (6) and (7) can be treated as a set of equations for $\nabla^2 T$ and $\nabla^2(Mc)$ which, when solved, leads to the following expressions

$$\nabla^2 T + \nabla \cdot \left[\lambda_T^*\nabla T + (\lambda_c/M)^*\nabla(Mc)\right] = 0, \tag{9}$$

$$\nabla^2(Mc) + \nabla \cdot \left[D_T^*\nabla T + (D_c/M)^*\nabla(Mc)\right] = 0, \tag{10}$$

where

$$\lambda_T^* = \frac{D_{cf}\lambda_T' - \lambda_{cf}D_T'}{D_{cf}\lambda_{Tf} - \lambda_{cf}D_{Tf}}, \quad (\lambda_c/M)^* = \frac{D_{cf}\lambda_c' - \lambda_{cf}D_c'}{D_{cf}\lambda_{Tf} - \lambda_{cf}D_{Tf}},$$

$$D_T^* = \frac{-D_{Tf}\lambda_T' + \lambda_{Tf}D_T'}{D_{cf}\lambda_{Tf} - \lambda_{cf}D_{Tf}}, \quad (D_c/M)^* = \frac{-D_{Tf}\lambda_c' - \lambda_{Tf}D_c'}{D_{cf}\lambda_{Tf} - \lambda_{cf}D_{Tf}}.$$

Next we introduce Green's function defined by

$$\begin{aligned} &\nabla^2 G(\boldsymbol{x}, \boldsymbol{y}) + \delta(\boldsymbol{x}, \boldsymbol{y}) = 0 \quad \text{in } V, \\ &G(\boldsymbol{x}, \boldsymbol{y}) = 0 \quad \text{on } A, \end{aligned} \tag{11}$$

where $\delta(\boldsymbol{x}, \boldsymbol{y})$ is Dirac delta function and V and A are the volume and the surface of the medium, respectively.

If the second term on the left-hand side of Eqs. (9) and (10) can be treated as the heat or solute source terms, then the solution of these equations can be formally written as

$$\begin{aligned} T(\boldsymbol{x}, \Omega) = &-\int_V \nabla G(\boldsymbol{x}, \boldsymbol{y}) \cdot \left[\lambda_T^*\nabla T(\boldsymbol{y}, \Omega) \right. \\ &\left. + (\lambda_c/M)^*\nabla Mc(\boldsymbol{y}, \Omega)\right] \mathrm{d}V \\ &- \int_A \nabla G(\boldsymbol{x}, \boldsymbol{y}) \cdot \boldsymbol{n} T(\boldsymbol{y}, \Omega)\, \mathrm{d}A, \end{aligned} \tag{12}$$

$$\begin{aligned} Mc(\boldsymbol{x}, \Omega) = &-\int_V \nabla G(\boldsymbol{x}, \boldsymbol{y}) \cdot \left[D_T^*\nabla T(\boldsymbol{y}, \Omega) \right. \\ &\left. + (D_c/M)^*\nabla Mc(\boldsymbol{y}, \Omega)\right] \mathrm{d}V \\ &- \int_A \nabla G(\boldsymbol{x}, \boldsymbol{y}) \cdot \boldsymbol{n} Mc(\boldsymbol{y}, \Omega)\, \mathrm{d}A, \end{aligned} \tag{13}$$

where $\boldsymbol{n}$ is the external unit vector perpendicular to A. After ensemble averaging of Eqs. (12) and (13), specifying the Dirichlet type boundary conditions for T and c on the external boundaries of the suspension and subtracting the result from Eqs. (12) and (13), the microscopic temperature T and the microscopic activity Mc can be expressed as

$$\begin{aligned} T(\boldsymbol{x}, \Omega) = \{T(\boldsymbol{x})\} - &\int_V \nabla G(\boldsymbol{x}, \boldsymbol{y}) \cdot \left[\left[\lambda_T^*\nabla T(\boldsymbol{y}, \Omega) \right.\right. \\ &\left. - \{\lambda_T^*\nabla T(\boldsymbol{y})\}\right] + \left[(\lambda_c/M)^*\nabla Mc(\boldsymbol{y}, \Omega) \right. \\ &\left.\left. - \{(\lambda_c/M)^*\nabla Mc(\boldsymbol{y})\}\right]\right] \mathrm{d}V, \end{aligned} \tag{14}$$

$$\begin{aligned} Mc(\boldsymbol{x}, \Omega) = \{Mc(\boldsymbol{x})\} - &\int_V \nabla G(\boldsymbol{x}, \boldsymbol{y}) \\ &\cdot \left[\left[D_T^*\nabla T(\boldsymbol{y}, \Omega) - \{D_T^*\nabla T(\boldsymbol{y})\}\right]\right. \\ &+ \left[(D_c/M)^*\nabla Mc(\boldsymbol{y}, \Omega) \right. \\ &\left.\left. - \{(D_c/M)^*\nabla Mc(\boldsymbol{y})\}\right]\right] \mathrm{d}V. \end{aligned} \tag{15}$$

We seek the solution of Eqs. (14) and (15) in the following form

$$T(\boldsymbol{x}) = \{T(\boldsymbol{x})\} + \int_V [\varphi_{TT}(\boldsymbol{x}, \boldsymbol{y}, \Omega)\nabla\{T(\boldsymbol{y})\} + \varphi_{Tc}(\boldsymbol{x}, \boldsymbol{y}, \Omega)\nabla\{Mc(\boldsymbol{y})\}]\, dV, \quad (16)$$

$$Mc(\boldsymbol{x}) = \{Mc(\boldsymbol{x})\} + \int_V [\varphi_{cT}(\boldsymbol{x}, \boldsymbol{y}, \Omega)\nabla\{T(\boldsymbol{y})\} + \varphi_{cc}(\boldsymbol{x}, \boldsymbol{y}, \Omega)\nabla\{Mc(\boldsymbol{y})\}]dV. \quad (17)$$

Equations for the unknown vector functions φ_{TT}, φ_{Tc}, φ_{cT} and φ_{cc} (microstructure functions) can be found by substitution of the above relations into Eqs. (14) and (15) and demonstrating that the resultant equations are independent of the macroscopic fields $\{T\}$ and $\{Mc\}$. This procedure results in the following expressions

$$\varphi_{TT}(\boldsymbol{x}, \Omega) = -\int_V \nabla G(\boldsymbol{x}, \boldsymbol{y}) \cdot \Big[\big[\lambda_T^*(\delta\mathbf{1} + \nabla\varphi_{TT}) - \{\lambda_T^*(\delta\mathbf{1} + \nabla\varphi_{TT})\}\big] + \big[(\lambda_c/M)^*\nabla\varphi_{cT} - \{(\lambda_c/M)^*\nabla\varphi_{cT}\}\big]\Big]\, dV, \quad (18)$$

$$\varphi_{Tc}(\boldsymbol{x}, \Omega) = -\int_V \nabla G(\boldsymbol{x}, \boldsymbol{y}) \cdot \Big[\big[\lambda_T^*\nabla\varphi_{Tc} - \{\lambda_T^*\nabla\varphi_{Tc}\}\big] + \big[(\lambda_c/M)^*(\delta\mathbf{1} + \nabla\varphi_{cc}) - \{(\lambda_c/M)^*(\delta\mathbf{1} + \nabla\varphi_{cc})\}\big]\Big]\, dV, \quad (19)$$

$$\varphi_{cT}(\boldsymbol{x}, \Omega) = -\int_V \nabla G(\boldsymbol{x}, \boldsymbol{y}) \cdot \Big[\big[D_T^*(\delta\mathbf{1} + \nabla\varphi_{TT}) - \{D_T^*(\delta\mathbf{1} + \nabla\varphi_{TT})\}\big] + \big[(D_c/M)^*\nabla\varphi_{cT} - \{(D_c/M)^*\nabla\varphi_{cT}\}\big]\Big]\, dV, \quad (20)$$

$$\varphi_{cc}(\boldsymbol{x}, \Omega) = -\int_V \nabla G(\boldsymbol{x}, \boldsymbol{y}) \cdot \Big[\big[D_T^*\nabla\varphi_{Tc} - \{D_T^*\nabla\varphi_{Tc}\}\big] + \big[(D_c/M)^*(\delta\mathbf{1} + \nabla\varphi_{cc}) - \{(D_c/M)^*(\delta\mathbf{1} + \nabla\varphi_{cc})\}\big]\Big]\, dV, \quad (21)$$

where $\mathbf{1}$ denotes the unit second order tensor.

2.3. Constitutive relations

When the relations between microscopic and macroscopic temperature and activity fields (Eqs. (16) and (17)) are known, it is easy to obtain relations between the mean (macroscopic) heat flux and the mean (macroscopic) mass flux, on one side, and the mean (macroscopic) temperature and the mean (macroscopic) solute concentration, on the other side. This can be simply achieved by substitution of Eqs. (16) and (17) and Eq. (A6) from Appendix A into Eq. (5)

$$-\{\boldsymbol{q}(\boldsymbol{x})\} = \int_V \lambda_T^{ef}(\boldsymbol{x}, \boldsymbol{y}) \cdot \nabla\{T(\boldsymbol{y})\}\, dV + \int_V \lambda_c^{ef}(\boldsymbol{x}, \boldsymbol{y}) \cdot \nabla\{c(\boldsymbol{y})\}\, dV, \quad (22)$$

$$-\{\boldsymbol{j}(\boldsymbol{x})\} = \int_V D_T^{ef}(\boldsymbol{x}, \boldsymbol{y}) \cdot \nabla\{T(\boldsymbol{y})\}\, dV + \int_V D_c^{ef}(\boldsymbol{x}, \boldsymbol{y}) \cdot \nabla\{c(\boldsymbol{y})\}\, dV, \quad (23)$$

where the effective thermal conductivity λ_T^{ef}, effective Dufour coefficient λ_c^{ef}, effective Soret coefficient D_c^{ef} and effective solute diffusivity D_T^{ef} are defined by the expressions

$$\lambda_T^{ef} = \{\lambda_T(\delta\mathbf{1} + \nabla\varphi_{TT})\} + \{\lambda_c\nabla\varphi_{cT}\},$$

$$\lambda_c^{ef} = \{\lambda_T MP_{eq}\nabla\varphi_{Tc}\} + \{\lambda_c MP_{eq}(\delta\mathbf{1} + \nabla\varphi_{cc})\},$$

$$D_T^{ef} = \{D_T(\delta\mathbf{1} + \nabla\varphi_{TT})\} + \{D_c\nabla\varphi_{cT}\},$$

$$D_c^{ef} = \{D_T MP_{eq} + \nabla\varphi_{Tc}\} + \{D_c MP_{eq}(\delta\mathbf{1} + \nabla\varphi_{cc})\}, \quad (24)$$

where P_{eq} stands for the concentration equilibrium distribution function.

The constitutive relations, Eqs. (22) and (23), are nonlocal. The macroscopic heat (or mass) flux for any location $\boldsymbol{x}$ in the suspension depends not only on the macroscopic temperature gradient and the macroscopic concentration gradient in the same location, but also on the distribution of these gradients for all other locations $\boldsymbol{y}$ in the medium.

In general, the effective material functions do not describe the effective properties of the medium; they describe the effective properties of the suspension only in these locations where they are not affected by the presence of the boundaries of the medium.

2.4. Expansions for the slowly varying fields

If the macroscopic temperature in the suspension is varying slowly in comparison with the microscopic variation of the medium properties, expansions of the following type [20] can be utilized

$$\varphi_{TT}(\boldsymbol{x}, \boldsymbol{y}) = [\varphi_{TT}^*(\boldsymbol{x}) - x]\delta(\boldsymbol{x}, \boldsymbol{y}) + l\varphi_{TT}^{**}(\boldsymbol{x}) \cdot \nabla\delta(\boldsymbol{x}, \boldsymbol{y}) + \cdots,$$

$$\varphi_{Tc}(\boldsymbol{x}, \boldsymbol{y}) = \varphi_{Tc}^*(\boldsymbol{x})\delta(\boldsymbol{x}, \boldsymbol{y}) + l\varphi_{Tc}^{**}(\boldsymbol{x}) \cdot \nabla\delta(\boldsymbol{x}, \boldsymbol{y}) + \cdots,$$

$$\varphi_{cT}(\boldsymbol{x},\boldsymbol{y}) = \varphi^{*}_{cT}(\boldsymbol{x})\delta(\boldsymbol{x},\boldsymbol{y}) + l\varphi^{**}_{cT}(\boldsymbol{x})\cdot\nabla\delta(\boldsymbol{x},\boldsymbol{y}) + \cdots,$$

$$\varphi_{cc}(\boldsymbol{x},\boldsymbol{y}) = \left[\varphi^{*}_{cc}(\boldsymbol{x}) - x\right]\delta(\boldsymbol{x},\boldsymbol{y}) + l\varphi^{**}_{cc}(\boldsymbol{x})\cdot\nabla\delta(\boldsymbol{x},\boldsymbol{y}) + \cdots, \tag{25}$$

for each of the functions φ_{TT}, φ_{Tc}, φ_{cT}, φ_{cc}. Symbol l here stands for the characteristic microdimension in the heterogeneous medium [8].

When these expansions are truncated after the first term and substituted into Eqs. (22) and (23), the constitutive relations reduce to the local relations, similar in form to the two relations given in Eq. (1), i.e.,

$$-\{\boldsymbol{q}(\boldsymbol{x})\} = \lambda^{ef*}_{T}(\boldsymbol{x})\cdot\nabla\{T(\boldsymbol{x})\} + \lambda^{ef*}_{c}(\boldsymbol{x})\cdot\nabla\{c(\boldsymbol{x})\},$$

$$-\{\boldsymbol{j}(\boldsymbol{x})\} = D^{ef*}_{T}(\boldsymbol{x})\cdot\nabla\{T(\boldsymbol{x})\} + D^{ef*}_{c}(\boldsymbol{x})\cdot\nabla\{c(\boldsymbol{x})\}. \tag{26}$$

The effective material functions (tensors) assume the following form

$$\lambda^{ef*}_{T} = \lambda_{Tf}\mathbf{1} + \lambda'_{Tp}\{(\theta\nabla\varphi^{*}_{TT})\} + \lambda'_{cp}\{\theta\nabla\varphi^{*}_{cT}\},$$

$$\lambda^{ef*}_{c} = \lambda_{cf}MP_{eq}\mathbf{1} + (\lambda_{Tp}MP_{eq})'\{(\theta\nabla\varphi^{*}_{Tc})\} + (\lambda_{cp}MP_{eq})'\{\theta\nabla\varphi^{*}_{cc}\},$$

$$D^{ef*}_{T} = D_{Tf}\mathbf{1} + D'_{Tp}\{(\theta\nabla\varphi^{*}_{TT})\} + D'_{cp}\{\theta\nabla\varphi^{*}_{cT}\},$$

$$D^{ef*}_{c} = D_{cf}MP_{eq}\mathbf{1} + (D_{Tp}MP_{eq})'\{(\theta\nabla\varphi^{*}_{Tc})\} + (D_{cp}MP_{eq})'\{\theta\nabla\varphi^{*}_{cc}\}. \tag{27}$$

where λ^{ef*}_{T}, λ^{ef*}_{c}, D^{ef*}_{T} and D^{ef*}_{T} are the effective thermal conductivity, effective Dufour coefficient, effective Soret coefficient and effective solute diffusivity, respectively, corresponding to the first term of expansions, Eq. (25). The integro-differential equations, Eqs. (18)–(21), are also simplified by introducing the above expansions and can be written as

$$\varphi^{*}_{TT}(\boldsymbol{x},\Omega) = \boldsymbol{x} - \int_{V}\nabla G(\boldsymbol{x},\boldsymbol{y})\cdot\Big[\left[\lambda^{*}_{T}\nabla\varphi^{*}_{TT} - \{\lambda^{*}_{T}\nabla\varphi^{*}_{TT}\}\right] + \left[(\lambda_{c}/M)^{*}\nabla\varphi^{*}_{cT} - \{(\lambda_{c}/M)^{*}\nabla\varphi^{*}_{cT}\}\right]\Big]\,dV, \tag{28}$$

$$\varphi^{*}_{Tc}(\boldsymbol{x},\Omega) = -\int_{V}\nabla G(\boldsymbol{x},\boldsymbol{y})\cdot\Big[\left[\lambda^{*}_{T}\nabla\varphi^{*}_{Tc} - \{\lambda^{*}_{T}\nabla\varphi^{*}_{Tc}\}\right] + \left[(\lambda_{c}/M)^{*}\nabla\varphi^{*}_{cc} - \{(\lambda_{c}/M)^{*}\nabla\varphi^{*}_{cc}\}\right]\Big]\,dV, \tag{29}$$

$$\varphi^{*}_{cT}(\boldsymbol{x},\Omega) = -\int_{V}\nabla G(\boldsymbol{x},\boldsymbol{y})\cdot\Big[\left[D^{*}_{T}\nabla\varphi^{*}_{TT} - \{D^{*}_{T}\nabla\varphi^{*}_{TT}\}\right] + \left[(D_{c}/M)^{*}\nabla\varphi^{*}_{cT} - \{(D_{c}/M)^{*}\nabla\varphi^{*}_{cT}\}\right]\Big]\,dV, \tag{30}$$

$$\varphi^{*}_{cc}(\boldsymbol{x},\Omega) = -\int_{V}\nabla G(\boldsymbol{x},\boldsymbol{y})\cdot\Big[\left[D^{*}_{T}\nabla\varphi^{*}_{Tc} - \{D^{*}_{T}\nabla\varphi^{*}_{Tc}\}\right] + \left[(D_{c}/M)^{*}\nabla\varphi^{*}_{cc} - \{(D_{c}/M)^{*}\nabla\varphi^{*}_{cc}\}\right]\Big]\,dV. \tag{31}$$

In the case of a heterogeneous medium, considered here, one of the constituents exists in the form of separate particles. The volume integrals, appearing on the right-hand sides of Eqs. (28)–(31), are nonzero only in the particles. After using Green's theorem for changing from volume to surface integrals, Eqs (28)–(30) take the following form

$$\begin{aligned}&\varphi^{*}_{TT} + \lambda^{*}_{Tp}\oint_{A_1} G\nabla\varphi^{*}_{TT}\cdot\boldsymbol{n}\,dA_1 + \lambda^{*}_{cp}\oint_{A_1} G\nabla\varphi^{*}_{cT}\cdot\boldsymbol{n}\,dA_1 + \sum_{j=2}\left[\lambda^{*}_{Tp}\oint_{A_j} G\nabla\varphi^{*}_{TT}\cdot\boldsymbol{n}\,dA_j + \lambda^{*}_{cp}\oint_{A_j} G\nabla\varphi^{*}_{cT}\cdot\boldsymbol{n}\,dA_j\right]\\ &= \boldsymbol{x} + \lambda^{*}_{Tp}\oint_{A} G\{\theta\nabla\varphi^{*}_{TT}\}\cdot\boldsymbol{n}\,dA + \lambda^{*}_{cp}\oint_{A} G\{\theta\nabla\varphi^{*}_{cT}\}\cdot\boldsymbol{n}\,dA,\end{aligned} \tag{32}$$

$$\begin{aligned}&\varphi^{*}_{Tc} + \lambda^{*}_{Tp}\oint_{A_1} G\nabla\varphi^{*}_{Tc}\cdot\boldsymbol{n}\,dA_1 + \lambda^{*}_{cp}\oint_{A_1} G\nabla\varphi^{*}_{cc}\cdot\boldsymbol{n}\,dA_1 + \sum_{j=2}\left[\lambda^{*}_{Tp}\oint_{A_j} G\nabla\varphi^{*}_{Tc}\cdot\boldsymbol{n}\,dA_j + \lambda^{*}_{cp}\oint_{A_j} G\nabla\varphi^{*}_{cc}\cdot\boldsymbol{n}\,dA_j\right]\\ &= \lambda^{*}_{Tp}\oint_{A} G\{\theta\nabla\varphi^{*}_{Tc}\}\cdot\boldsymbol{n}\,dA + \lambda^{*}_{cp}\oint_{A} G\{\theta\nabla\varphi^{*}_{cc}\}\cdot\boldsymbol{n}\,dA,\end{aligned} \tag{33}$$

$$\varphi^*_{cT} + D^*_{Tp}\oint_{A_1} G\nabla\varphi^*_{TT}\cdot\boldsymbol{n}\,dA_1 + D^*_{cp}\oint_{A_1} G\nabla\varphi^*_{cT}\cdot\boldsymbol{n}\,dA_1 + \sum_{j=2}\left[D^*_{Tp}\oint_{A_j} G\nabla\varphi^*_{TT}\cdot\boldsymbol{n}\,dA_j + D^*_{cp}\oint_{A_j} G\nabla\varphi^*_{cT}\cdot\boldsymbol{n}\,dA_j\right] = D^*_{Tp}\oint_{A} G\{\theta\nabla\varphi^*_{TT}\}\cdot\boldsymbol{n}\,dA + D^*_{cp}\oint_{A} G\{\theta\nabla\varphi^*_{cT}\}\cdot\boldsymbol{n}\,dA, \tag{34}$$

$$[\varphi^*_{cc} + D^*_{Tp}\oint_{A_1} G\nabla\varphi^*_{Tc}\cdot\boldsymbol{n}\,dA_1 + D^*_{cp}\oint_{A_1} G\nabla\varphi^*_{cc}\cdot\boldsymbol{n}\,dA_1 + \sum_{j=2}\left[D^*_{Tp}\oint_{A_j} G\nabla\varphi^*_{Tc}\cdot\boldsymbol{n}\,dA_j + D^*_{cp}\oint_{A_j} G\nabla\varphi^*_{cc}\cdot\boldsymbol{n}\,dA_j\right] = \boldsymbol{x} + D^*_{Tp}\oint_{A} G\{\theta\nabla\varphi^*_{Tc}\}\cdot\boldsymbol{n}\,dA + D^*_{cp}\oint_{A} G\{\theta\nabla\varphi^*_{cc}\}\cdot\boldsymbol{n}\,dA. \tag{35}$$

On solving Eqs. (32)–(35) we can obtain functions φ_{TT}, φ_{Tc}, φ_{cT} and φ_{cc} for any location in the medium (either inside the particles or inside the fluid) for any distribution of the particles in the suspension. The second and third terms on the left-hand sides of these equations describe the influence of the particle that is the closest to the considered location. The fourth term gives influence of other, more distant particles. The right-hand sides of these equations are independent of any particular distribution of the particles and is related to the mean temperature and concentration fields in the medium.

The standard solution of these equations consists of considering, in sequence, the influence of more and more distant particles on the functions φ_{TT}, φ_{Tc}, φ_{cT} and φ_{cc}, starting with the closest one (the first one). Usually this influence quickly diminishes if the volume fraction of the particles in the suspension is small and when clustering of the particles is absent. This approach will be followed in the subsequent considerations. It is worth to note here that addition of any new particle in the medium will modify the right-hand sides of Eqs. (32)–(35).

3. Heat and solute flow through a barrier

3.1. Description of the barrier

Let us consider a barrier consisting of a suspension layer of thickness Δ that extends to infinity in the remaining directions (Fig. 1). The suspension is made of a carrier fluid with randomly distributed axi-symmetric particles. The particles have spheroidal shape with length L and radius R so that their aspect ratio is $\varepsilon^* = L/(2R)$. By varying the particle aspect ratio different shapes of the particles may be obtained, ranging from flattened disk-like particles (oblate spheroids with $\epsilon^* < 1$), to spheres ($\varepsilon^* = 1$), to elongated rod-like particles (prolate spheroids with $\varepsilon^* > 1$). It is assumed that the axes of symmetry of the particles are parallel to each other with their orientations described by angle γ (Fig. 1a). This orientation can be changed by external means (e.g., by applying electric or magnetic field [21]). The volume fraction of the particles is assumed to be sufficiently small to permit their free rotation.

Simultaneous heat conduction and solute diffusion take place in the suspension. The processes are coupled and either heat or mass flow may occur due to difference of temperature ($T_1 > T_2$) or due to difference of

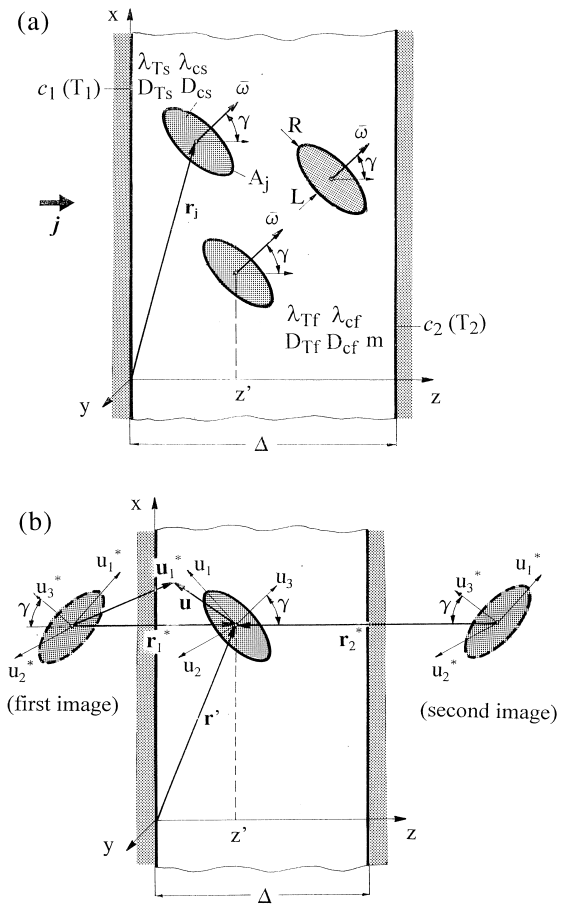

Fig. 1. A schematic diagram of the barrier that can be used for control of heat and solute flow.

concentrations of the solute ($c_1 > c_2$) on the opposite faces of the barrier. The solution of the diffusing species is treated as dilute so that locally Fick's law is applicable. It is further assumed that the whole system is in a steady state and that no convection occurs.

The main objective of this paper is to study how orientation of the particles affects the solute flux as a function of different parameters characterizing the barrier and as a function of different ways of forcing the solute flow (concentration difference or temperature difference). The relevant parameters are: (i) material parameters, like $\lambda_{Ts}/\lambda_{Tf}$, D_{cs}/D_{cf}, $\lambda_{cs}/\lambda_{cf}$, D_{Ts}/D_{Tf}, $\lambda_{cf}/\lambda_{Tf}$, D_{Tf}/D_{cf}, m; (ii) structural parameters, like class of particle shapes (disk-like and rod like), particle aspect ratio ε, particle volume fraction v, angle γ of orientation of particles, and (iii) geometrical parameters, like $\Delta/(2R)$. As the influence of some parameters was found to be similar to the previously studied pure heat conduction problem [3,4], a special attention has been focused on the parameters affecting mass diffusion and those affecting coupling between heat conduction and mass diffusion.

The problem of solute flow through a barrier is three-dimensional (on the microscopic level) due to complicated structure of the suspension. The advantage of studying this problem using the effective medium approach is that it reduces the original problem to a one-dimensional one on the macroscopic level. Eq. (26) can be simplified to the following form

$$-\{q\} = \lambda^{ef}_{T\perp}(z)\frac{d\{T\}}{dz} + \lambda^{ef}_{c\perp}(z)\frac{d\{c\}}{dz}, \tag{36}$$

$$-\{j\} = D^{ef}_{T\perp}(z)\frac{d\{T\}}{dz} + D^{ef}_{c\perp}(z)\frac{d\{c\}}{dz}, \tag{37}$$

where $\{q\}$, $\{j\}$ stand for the macroscopic heat and solute fluxes in the direction of the bulk flow (direction z) and symbol $\perp$ denotes components of the respective effective material tensors in the same direction.

3.2. Effective material tensors

In order to calculate either the heat or solute flow through the barrier, it is necessary to know the effective material tensors appearing in Eqs. (37) and (38). As noted earlier, these tensors become effective properties of the suspension at a certain distance away from the barrier faces. In deriving relations for the components of these tensors, we will follow a procedure which parallels the approach used in the study of pure heat conduction problem. This will allow us to concentrate on the main assumptions and omit the laborious derivations discussed previously in detail [3].

Firstly, let us note that due to the form of expressions for the material tensors, Eq. (27), only gradients of the microstructure functions are needed (the characteristic function θ is zero outside the particles). These functions have a linear form in the case of an infinite medium. Since our interest is only in the case of small volume fraction of spherical particles, we assume that these functions may retain a linear form even for a bounded medium. We, therefore, write these functions in the form

$$\varphi^*_{TT} = \boldsymbol{C}^0_{TT} + \boldsymbol{C}_{TT}\cdot\boldsymbol{u}_j, \quad \varphi^*_{Tc} = \boldsymbol{C}^0_{Tc} + \boldsymbol{C}_{Tc}\cdot\boldsymbol{u}_j,$$

$$\varphi^*_{cT} = \boldsymbol{C}^0_{cT} + \boldsymbol{C}_{cT}\cdot\boldsymbol{u}_j, \quad \varphi^*_{cc} = \boldsymbol{C}^0_{cc} + \boldsymbol{C}_{cc}\cdot\boldsymbol{u}_j, \tag{38}$$

where $\boldsymbol{u}_j = \boldsymbol{x} - \boldsymbol{r}_j$ and $\boldsymbol{r}_j$ stand for the position vectors associated with the center of the jth particle (Fig. 1). The assumption had been found to be strictly valid for any distribution of spheroidal particles when their volume fraction was small and when the gradient of macroscopic temperature $\{T\}$ was kept constant [20]. One should note, however, that the microstructure functions may be nonlinear outside the particles.

Secondly, since our interest is in the case of small volume fraction of the particles, we shall omit the fourth term on the left-hand sides of Eqs. (32)–(35). This means that only the influence of the first (i.e., the closest) particle on the microstructure function in the location $\boldsymbol{x}$ is retained. This assumption may need additional explanations. In order to study the influence of the interparticle interactions on the heat or mass fluxes, a number of investigators employed expansions of the temperature and/or concentration fields in terms of the particle volume fraction v (or more correctly, expansions in terms of a product of the number density of the particles and a cube of the largest dimension of the particle). They concluded that the second term in the expansion (the first order in v) corresponds to an isolated particle while the higher terms take account of the particle interactions. Some numerical simulations [10] show that results based on the two-term expansions are valid only for very small values of v (2–4% for spherical particles, with the more restrictive values for non-spherical ones). These results give rise to claims that validity of analyses based on two-term expansions (the single particle model) should be limited to these very low volume fractions. Numerical simulations for ordered arrays of particles as well as experimental results contradict these conclusions. Validity of, for example, Maxwell formula (spherical particles) or Rayleigh formula (cylindrical infinite fibers), which are derived from solution of a single particle problem, was found to be much broader with respect to v [20]. The reason for this behavior is known and is related to the manner in which the particles may interact. They may interact directly, and this effect is described by the third term on the left-hand sides of Eqs. (32)–(35), and

indirectly by modifying the macroscopic temperature or concentration field around each particle. The integrals on the right-hand side of Eqs. (32)–(35) correspond to the latter form of interaction. Typically, in any analysis based on the expansions in terms of particle volume fraction, indirect interaction are excluded. This may lead to significant discrepancies between the results based on the one- (single particle) and multiterm expansions already for very small volume fractions. If both ways of interaction are included in the analysis, it is found that their relative importance depends on the form of distribution of the particles. If clustering of the particles occurs, direct interactions between the particles are dominant and a significant difference between the results based on the many particle analysis and the single particle analysis may be observed already at very small volume fractions. But if no clustering occurs, i.e., the particles are well separated as, for example, in the ordered arrays of particles, then the indirect way of interaction is more important except for very high volume fractions of the particles. In the present case, the particles are well separated and thus the direct interactions can be omitted without limiting the validity of the results to extremely small volume fractions.

Equations for the unknown tensors $\boldsymbol{C}_{\mathrm{TT}}$, $\boldsymbol{C}_{\mathrm{Tc}}$, $\boldsymbol{C}_{\mathrm{cT}}$ and $\boldsymbol{C}_{\mathrm{cc}}$ can be found by substituting Eq. (38) into Eqs. (32)–(35) and specifying the location vector $\boldsymbol{x}$ for the microstructure functions to correspond to the interior of the particle. The resulting surface integrals have the form

$$\oint_{A_1} G\boldsymbol{n}\,\mathrm{d}A_1 = \boldsymbol{P}\cdot\left[\boldsymbol{u}_1 - \boldsymbol{F}(\boldsymbol{u}_1)\right], \tag{39}$$

where $\boldsymbol{P}$ is the Eshelby shape tensor solely dependent on the shape of the particle and on its aspect ratio. The form of the vector function $\boldsymbol{F}$ follows from application of the method of reflections [3] for deriving an appropriate expression for the Green function G and it is defined as

$$\begin{aligned}\boldsymbol{F}(\boldsymbol{u}) = \sum_{k=0}^{\infty}\Big[&\boldsymbol{f}\left(\boldsymbol{u}+\boldsymbol{r}_k^*;\,2k\Delta+2z'\right)\\ &+f\left(\boldsymbol{u}+\boldsymbol{r}_k^*;\,2(k+1)\Delta-2z'\right)\Big]\\ &-\sum_{k=1}^{\infty}\Big[f\left(\boldsymbol{u}+\boldsymbol{r}_k^*;\,2k\Delta\right)+f\left(\boldsymbol{u}+\boldsymbol{r}_k^*;\,2(k+1)\Delta\right)\Big],\end{aligned}$$

where $\boldsymbol{r}_k^*$ is a vector connecting the center of the kth image with the center of the considered particle, z' is the location of the center of the considered particle in the barrier (Fig. 1b) and the vector function $\boldsymbol{f}$ is related to the form of the microstructure function outside the particle placed in an infinite medium [3]. The detailed formulae for the function $\boldsymbol{f}$ are given in [10].

The explicit, analytical expressions for the tensors $\boldsymbol{C}_{\mathrm{TT}}$, $\boldsymbol{C}_{\mathrm{Tc}}$, $\boldsymbol{C}_{\mathrm{cT}}$ and $\boldsymbol{C}_{\mathrm{cc}}$ can be obtained by linearizing the function $\boldsymbol{F}$ with respect to $\boldsymbol{u}$, i.e.,

$$\boldsymbol{F}(\boldsymbol{u}) = \boldsymbol{F}(\boldsymbol{0}) + \nabla\boldsymbol{F}(\boldsymbol{0})\cdot\boldsymbol{u} + \cdots.$$

This procedure resembles the so-called Rayleigh method [20] used for deriving the effective properties of the ordered arrays of spherical particles. It is also consistent with the linearity assumption used in Eq. (38).

After substitution of Eq. (39) into Eqs. (32)–(35) and matching terms of the same order in $\boldsymbol{u}$, the following system of four equations for the unknowns $\boldsymbol{C}_{\mathrm{TT}}$, $\boldsymbol{C}_{\mathrm{Tc}}$, $\boldsymbol{C}_{\mathrm{cT}}$ and $\boldsymbol{C}_{\mathrm{cc}}$ results

$$\begin{aligned}&\left(\boldsymbol{1}+\lambda_{\mathrm{Tp}}^*\boldsymbol{P}^*\right)\cdot\boldsymbol{C}_{\mathrm{TT}} + \lambda_{\mathrm{cp}}^*\boldsymbol{P}^*\cdot\boldsymbol{C}_{\mathrm{cT}}\\ &\quad= \boldsymbol{1}+\lambda_{\mathrm{Tp}}^*\left\{\theta\boldsymbol{P}^*\cdot\boldsymbol{C}_{\mathrm{TT}}\right\}+\lambda_{\mathrm{cp}}^*\left\{\theta\boldsymbol{P}^*\cdot\boldsymbol{C}_{\mathrm{cT}}\right\},\\ &D_{\mathrm{cp}}^*\boldsymbol{P}^*\cdot\boldsymbol{C}_{\mathrm{TT}} + \left(\boldsymbol{1}+D_{\mathrm{cp}}^*\boldsymbol{P}^*\right)\cdot\boldsymbol{C}_{\mathrm{cT}}\\ &\quad= D_{\mathrm{Tp}}^*\left\{\theta\boldsymbol{P}^*\cdot\boldsymbol{C}_{\mathrm{TT}}\right\}+D_{\mathrm{cp}}^*\left\{\theta\boldsymbol{P}^*\cdot\boldsymbol{C}_{\mathrm{cT}}\right\},\end{aligned} \tag{40}$$

$$\begin{aligned}&\lambda_{\mathrm{cp}}^*\boldsymbol{P}^*\cdot\boldsymbol{C}_{\mathrm{cc}} + \left(\boldsymbol{1}+\lambda_{\mathrm{Tp}}^*\boldsymbol{P}^*\right)\cdot\boldsymbol{C}_{\mathrm{Tc}}\\ &\quad= \lambda_{\mathrm{Tp}}^*\left\{\theta\boldsymbol{P}^*\cdot\boldsymbol{C}_{\mathrm{Tc}}\right\}+\lambda_{\mathrm{cp}}^*\left\{\theta\boldsymbol{P}^*\cdot\boldsymbol{C}_{\mathrm{cc}}\right\},\\ &D_{\mathrm{Tp}}^*\boldsymbol{P}^*\cdot\boldsymbol{C}_{\mathrm{Tc}} + \left(\boldsymbol{1}+D_{\mathrm{cp}}^*\boldsymbol{P}^*\right)\cdot\boldsymbol{C}_{\mathrm{cc}}\\ &\quad= \boldsymbol{1}+D_{\mathrm{Tp}}^*\left\{\theta\boldsymbol{P}^*\cdot\boldsymbol{C}_{\mathrm{Tc}}\right\}+D_{\mathrm{cp}}^*\left\{\theta\boldsymbol{P}^*\cdot\boldsymbol{C}_{\mathrm{cc}}\right\},\end{aligned} \tag{41}$$

where $\boldsymbol{P}^* = \boldsymbol{P}\cdot[1-\nabla\boldsymbol{F}(\boldsymbol{0})]$.

In the following sections we shall solve this set of equations and study the solute flow through the barrier driven by two types of external forces:

- concentration gradient for uncoupled mass and heat flow,
- temperature gradient for coupled mass and heat flow.

4. Solute flow driven by concentration gradient

For uncoupled mass and heat flow, the Dufour λ_{c} and Soret D_T coefficients are equal to zero. The constants associated with the thermal and diffusive properties of suspension constituents, Eqs. (9) and (10), assume the following form

$$\lambda_{\mathrm{Tp}}^* = \left(\lambda_{\mathrm{Tp}}-\lambda_{\mathrm{Tf}}\right)/\lambda_{\mathrm{Tf}} = \sigma_{\mathrm{TT}}-1, \quad \lambda_{\mathrm{cp}}^* = 0,$$

$$\lambda_{\mathrm{cp}}^* = 0, \quad D_{\mathrm{cp}}^* = \left(D_{\mathrm{cp}}/m - D_{\mathrm{cf}}\right)/D_{\mathrm{cf}} = \sigma_{\mathrm{cc}}/m - 1.$$

If we substitute the above relations into Eqs. (41) and (42), we find that tensors $\boldsymbol{C}_{\mathrm{Tc}}$ and $\boldsymbol{C}_{\mathrm{cT}}$ are equal to zero. The remaining equations for the tensors $\boldsymbol{C}_{\mathrm{TT}}$ and $\boldsymbol{C}_{\mathrm{cc}}$ are similar to each other and the equation for $\boldsymbol{C}_{\mathrm{TT}}$ is identical to the one found in the case of pure heat conduction studied before [3,4]. Noting that the right-hand sides of Eqs. (41) and (42) are independent of any particular distribution of the particles, we have solved these equations in a manner identical to that described in [3]. Finally, substitution of the tensors $\boldsymbol{C}_{\mathrm{TT}}$, $\boldsymbol{C}_{\mathrm{Tc}}$, $\boldsymbol{C}_{\mathrm{cT}}$ and $\boldsymbol{C}_{\mathrm{cc}}$ into definitions, Eq. (27), leads to the following formulae for the effective material functions

$$\lambda_{\mathrm{T}}^{*\mathrm{ef}}/\lambda_{\mathrm{Tf}} = \mathbf{1} + \sigma'_{\mathrm{TT}}\left\{\theta\left(\mathbf{1}+\sigma'_{\mathrm{TT}}\boldsymbol{P}^*\right)^{-1}\right\} \cdot \left[1-\sigma'_{\mathrm{TT}}\left\{\theta\boldsymbol{P}^*\left(\mathbf{1}+\sigma'_{\mathrm{TT}}\boldsymbol{P}^*\right)^{-1}\right\}\right]^{-1},$$

$$\lambda_{\mathrm{c}}^{*\mathrm{ef}} = 0,$$

$$D_{\mathrm{T}}^{*\mathrm{ef}} = 0,$$

$$D_{\mathrm{c}}^{*\mathrm{ef}}/D_{\mathrm{cf}} = \left(MP_{\mathrm{eq}}\right)\mathbf{1} + \sigma'_{\mathrm{cc}}\left\{\theta\boldsymbol{P}_{\mathrm{eq}}\left(\mathbf{1}+\sigma'_{\mathrm{cc}}\boldsymbol{P}^*\right)^{-1}\right\} \cdot \left[\mathbf{1}-\sigma'_{\mathrm{cc}}\left\{\theta\boldsymbol{P}^*\left(\mathbf{1}+\sigma'_{\mathrm{cc}}\boldsymbol{P}^*\right)^{-1}\right\}\right]^{-1},$$

where

$$\sigma'_{\mathrm{TT}} = \sigma_{\mathrm{TT}} - 1, \quad \sigma'_{\mathrm{cc}} = \sigma_{\mathrm{cc}}/m - 1.$$

The principal directions of the second order tensors $\boldsymbol{P}^*$ and $\boldsymbol{P}$ are usually different and this makes estimation of the components of $\lambda_{\mathrm{T}}^{\mathrm{ef}}$ and $D_{\mathrm{c}}^{\mathrm{ef}}$ in the direction perpendicular to the walls laborious. Nevertheless, after carrying out transformations of components of both tensors from the local coordinate system associated with the reference particle to the global coordinate system (x, y, z) defined by the walls of the barrier (Fig. 1), the components $\lambda_{\mathrm{T}\perp}^{\mathrm{ef}*}$, $D_{\mathrm{c}\perp}^{\mathrm{ef}*}$ of the effective material functions in the direction normal to the barrier become

$$\lambda_{\mathrm{T}\perp}^{\mathrm{ef}*}/\lambda_{\mathrm{Tf}} = 1 + \frac{\sigma'_{\mathrm{TT}}\left[\{\theta\Gamma_1\}\left(1-\sigma'_{\mathrm{TT}}\{\theta\Gamma_2\}\right) - \sigma'_{\mathrm{TT}}\{\theta\Gamma_3\}\{\theta\Gamma_4\}\right]}{\left[\left(1-\sigma'_{\mathrm{TT}}\{\theta\Gamma_2\}\right)\left(1-\sigma'_{\mathrm{TT}}\{\theta\Gamma_5\}\right) - \sigma'_{\mathrm{TT}}\{\theta\Gamma_4\}\{\theta\Gamma_6\}\right]}, \tag{42}$$

$$D_{\mathrm{c}\perp}^{\mathrm{ef}*}/D_{\mathrm{Tf}} = \left(MP_{\mathrm{eq}}\right) \left[1 + \frac{\sigma'_{\mathrm{cc}}\left[\{\theta\Gamma_1\}\left(1-\sigma'_{\mathrm{cc}}\{\theta\Gamma_2\}\right) - \sigma'_{\mathrm{cc}}\{\theta\Gamma_3\}\{\theta\Gamma_4\}\right]}{\left[\left(1-\sigma'_{\mathrm{cc}}\{\theta\Gamma_2\}\right)\left(1-\sigma'_{\mathrm{cc}}\{\theta\Gamma_5\}\right) - \sigma'_{\mathrm{cc}}\{\theta\Gamma_4\}\{\theta\Gamma_6\}\right]}\right], \tag{43}$$

with functions $\Gamma_1, \ldots, \Gamma_6$ given elsewhere [9]. The way of evaluation of the ensemble averages $\{\theta\Gamma_n\}$, $n = 1, \ldots, 6$, has also been described in detail in previous papers [3,9].

The local values of the effective material functions $\lambda_{\mathrm{T}\perp}^{\mathrm{ef}}$, $\lambda_{\mathrm{c}\perp}^{\mathrm{ef}}$, $D_{\mathrm{c}\perp}^{\mathrm{ef}}$, $D_{\mathrm{T}\perp}^{\mathrm{ef}}$ and the volume fraction of the particles v vary across the barrier. The variation of v can be determined from the formula: $v(z) = \{\theta\}$. Analysis of the distribution of the local volume fraction shows that it attains a maximum value v_{m} in the middle of the barrier and decreases to zero at the wall. When particles are oriented in such a way that their major axes are parallel to the wall, a layer of pure fluid separates them from the walls. Under such circumstances the local volume fraction falls to zero before reaching the wall. The assumed distribution of the particles leads to a strict relation between the maximum volume fraction v_{m} and the mean volume fraction $\tilde{v}$ [9]. As v_{m} is bounded from above by the assumption of the small local volume fraction, this relation places limitations on the mean particle volume fraction $\tilde{v}$ and on the ratio of the barrier thickness Δ to the length of the particle major axis.

As mentioned previously, the problem of pure heat flow through the barrier will not be considered here. We shall now begin discussion of new results by looking at the mass flow of the solute.

The bulk flow of the solute across the barrier, when concentrations c_1 and c_2 ($c_1 > c_2$) on both faces are given, can be evaluated from the formula

$$\{j\} = (c_1 - c_2)/\int_0^{\Delta} \mathrm{d}z/D_{\mathrm{c}\perp}^{\mathrm{ef}*}(z) \tag{44}$$

which can be easily derived from Eq. (37). In order to estimate $D_{\mathrm{T}\perp}^{\mathrm{ef}*}(z)$, components of tensor $\boldsymbol{P}^*$ corresponding to a particular orientation of the particles, described by the angle γ, have been determined. Then all ensemble averaged quantities appearing in the formula (43) were calculated. Finally, the integration in Eq. (44) was carried out.

The mass flux of the solute diffusing through the barrier is influenced by both the microstructure of the suspension, properties of the constituents and thickness of the barrier. The structural parameters include the mean volume fraction v the particles, their orientation, aspect ratio and diameter as well as the class of shapes of the particles. The material parameters include particle/fluid diffusivity ratio and solubility.

The diffusivity of the solute for the solid particles is usually much smaller than for the fluid. So from two classes of particle shapes studied, we have found that the disk-like particles are significantly more effective in controlling the flow of the solute by changing orientation of the particles. Because of that we have focused most of our calculations on the disk-like particles. After studying the influence of angle γ of rotation of the particles, we have found that for the disk-like particles in all cases, the maximum value of the solute flux occurred for particle axes parallel to barrier faces while the minimum value occurred when particles were perpendicular. The opposite was found to be true for the rod-like particles. All results presented in this paper are in the form of a ratio of the maximum to the minimum flow of the solute. This ratio is a good measure of the effectiveness of the barrier in controlling the mass flow.

All material properties of the constituents have a significant effect on j_{max}/j_{min}. A decrease of the particle/fluid diffusivity ratio makes the barrier more effective (Fig. 2a). An increase of the particle/fluid solute solubility m results in an increase of the barrier effectiveness. The largest increase occurs for $D_{cs}/D_{cf} \approx 0.1/0.3$; it decreases when $D_{cs}/D_{cf} \to 1$ (Fig. 2a) as well as when $D_{cs}/D_{cf} \to 0$ (Fig. 2b).

The ratio of the barrier thickness Δ to the particle diameter $(2R)$ has a small impact on j_{max}/j_{min} and its role in controlling the solute flux seems almost unimportant for practical purposes (Fig. 3a). A slight increase in the barrier effectiveness has been observed when the barrier is made thinner as compared to the particle diameter.

The mean volume fraction $\tilde{v}$ the particles significantly influences the solute flow through the barrier (Fig. 3b). The greater the value of $\tilde{v}$, the broader the range of control of the magnitude of the solute flux.

Inverse of the particle aspect ratio $\varepsilon = (2R)/L$ appears to be the most important factor in controlling the solute flow. An increase of ε leads to broadening of the range in which the solute flow may be controlled by the particle rotation (Fig. 4a). The relation between j_{max}/j_{min} and ε has been found to be almost linear.

The assumption of space availability for rotation of the particles in the fluid places additional limitation on the maximum value of the mean particle volume fraction. This condition, for the disk-like particles, can be written as $v_{max} \leq (1/\varepsilon)$ and, if we assume that the admissible particle volume fraction is congruent with this condition, then the ratio j_{max}/j_{min} varies differently with the aspect ratio of the particles (Fig. 4b). The effectiveness of the barrier for higher values of $\tilde{v}$ is now much lower and for $\varepsilon > 10$ it attains an asymptotic value.

5. Solute flow driven by temperature gradient

As an alternative way of controlling mass flow through the barrier, we shall consider the case when concentration of the diffusing species is the same at both faces of the barrier and the solute flow is driven only by a temperature difference. This time Defour and Soret coefficients are not equal to zero. As has been discussed in the previous section, the maximum

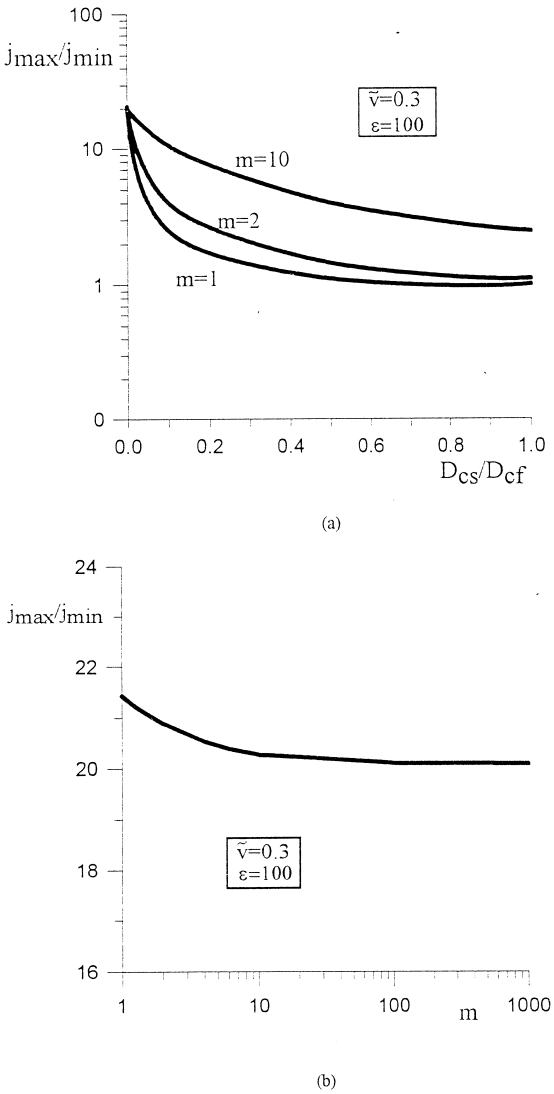

Fig. 2. Variation of the barrier effectiveness, defined as ratio of the maximum possible solute flux j_{max} and the minimum possible solute flux j_{min}, as a function of (a) particle/fluid diffusivity ratio $D_{cs}/D_{cf} > 0$ and solubility m, (b) solubility m for $D_{cs} = 0$. The reader should note that change of solute flux from j_{max} to j_{min} occurs due to change in orientation of the suspended particles.

and the minimum mass flows occur for orientations of the particles corresponding to the axes of symmetry of the particles being either perpendicular or parallel to the faces of the barrier.

For both perpendicular as well as parallel orientations of the particle tensors $\boldsymbol{P}$ and $\boldsymbol{P}^*$ as well as tensors $\boldsymbol{C}_{\mathrm{TT}}$, $\boldsymbol{C}_{\mathrm{Tc}}$, $\boldsymbol{C}_{\mathrm{cT}}$ and $\boldsymbol{C}_{\mathrm{cc}}$ have the same orientation of the principal axes. We solve Eqs. (40) and (41) for each principal component of these tensors separately and then write the expressions for the effective material constants in the direction normal to the barrier as follows

$$\begin{aligned}
\lambda^{\mathrm{ef}}_{\mathrm{T}\perp}/\lambda_{\mathrm{Tf}} &= 1+\sigma'_{\mathrm{TT}}\{\theta\boldsymbol{C}_{\mathrm{TT}}\}+\kappa_{\mathrm{T}}\sigma'_{\mathrm{cT}}\{\theta\boldsymbol{C}_{\mathrm{cT}}\},\\
D^{\mathrm{ef}}_{\mathrm{T}\perp}/D_{\mathrm{cf}} &= \kappa_{\mathrm{c}}+\kappa_{\mathrm{c}}\sigma'_{\mathrm{Tc}}\{\theta\boldsymbol{C}_{\mathrm{TT}}\}+\sigma'_{\mathrm{cc}}\{\theta\boldsymbol{C}_{\mathrm{cT}}\},\\
\lambda^{\mathrm{ef}}_{\mathrm{c}\perp}/\lambda_{\mathrm{Tf}} &= (MP_{\mathrm{eq}})[\kappa_{\mathrm{T}}+\kappa_{\mathrm{T}}\sigma'_{\mathrm{cT}}\{\theta\boldsymbol{C}_{\mathrm{cc}}\}+\sigma'_{\mathrm{TT}}\{\theta\boldsymbol{C}_{\mathrm{Tc}}\}],\\
D^{\mathrm{ef}}_{\mathrm{c}\perp}/D_{\mathrm{cf}} &= (MP_{\mathrm{eq}})[1+\sigma'_{\mathrm{cc}}\{\theta\boldsymbol{C}_{\mathrm{cc}}\}+\kappa_{\mathrm{c}}\sigma'_{\mathrm{Tc}}\{\theta\boldsymbol{C}_{\mathrm{Tc}}\}],
\end{aligned} \tag{45}$$

where

$$\sigma_{\mathrm{cT}}=\lambda_{\mathrm{cs}}/\lambda_{\mathrm{cf}},\quad \sigma'_{\mathrm{cT}}=\sigma_{\mathrm{cT}}/m-1,$$

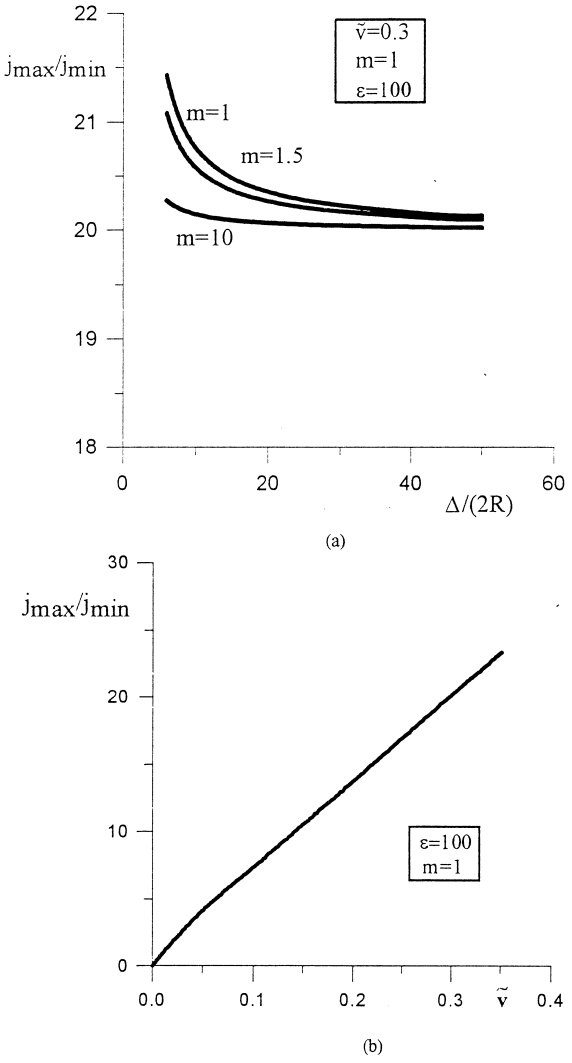

Fig. 3. Variation of the barrier effectiveness $j_{\max}/j_{\min}$ for $D_{\mathrm{cs}}=0$ as a function of (a) the barrier thickness $\Delta/(2R)$, (b) particle volume fraction $\tilde{v}$. (See Fig. 2 for additional explanations.)

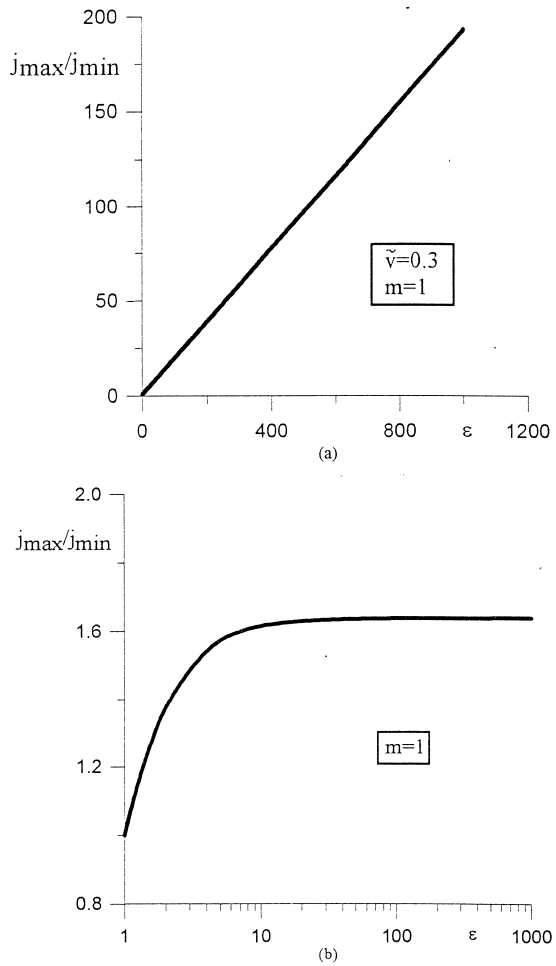

Fig. 4. Variation of the barrier effectiveness $j_{\max}/j_{\min}$ for $D_{\mathrm{cs}}=0$ as a function of the particle aspect ratio ε (a) for the volume fraction $\tilde{v}$ independent of ε, (b) for the maximum value of $\tilde{v}$ dependent on ε. Estimates of the latter case quarantee that the particles have enough free space to permit their rotation.

$$\sigma_{Tc} = D_{Ts}/D_{Tf}, \quad \sigma'_{Tc} = \sigma_{Tc} - 1,$$

$$\kappa_T = \lambda_{cf}/\lambda_{Tf}, \quad \kappa_c = D_{Tf}/D_{cf}, \tag{46}$$

and $\boldsymbol{C}_{TT}$, $\boldsymbol{C}_{Tc}$, $\boldsymbol{C}_{cT}$ and $\boldsymbol{C}_{cc}$ stand for components of the respective tensors in the direction z. These components may be calculated from the following formulae

$$\boldsymbol{C}_{TT} = \left(1 + D^*_{cp}\boldsymbol{P}^*\right)B_1/H - \left(\lambda^*_{cp}\boldsymbol{P}^*\right)B_2/H,$$

$$\boldsymbol{C}_{cT} = -\left(D^*_{Tp}\boldsymbol{P}^*\right)B_1/H + \left(1 + \lambda^*_{Tp}\boldsymbol{P}^*\right)B_2/H,$$

$$\boldsymbol{C}_{Tc} = -\left(\lambda^*_{cp}\boldsymbol{P}^*\right)B_4/H + \left(1 + D^*_{cp}\boldsymbol{P}^*\right)B_3/H,$$

$$\boldsymbol{C}_{cc} = \left(1 + \lambda^*_{Tp}\boldsymbol{P}^*\right)B_4/H - \left(D^*_{Tp}\boldsymbol{P}^*\right)B_3/H,$$

where

$$H = 1 + \left(\lambda^*_{Tp} + D^*_{cp}\right)\boldsymbol{P}^* + \left(\lambda^*_{Tp}D^*_{cp} - \lambda^*_{cp}D^*_{Tp}\right)(\boldsymbol{P}^*)^2,$$

$$B_1 = E_2/(E_1E_2 - E_3E_4), \quad B_2 = E_4/(E_1E_2 - E_3E_4),$$

$$B_3 = E_3/(E_1E_2 - E_3E_4), \quad B_4 = E_1/(E_1E_2 - E_3E_4),$$

The constants E_1, E_2, E_3 and E_4, appearing in the above formulae, are related to the ensemble averaged (macroscopic quantities) by the expressions

$$E_1 = 1 - \boldsymbol{P}^*\left[\lambda^*_{Tp} - g\boldsymbol{P}^*\right]v/H,$$

$$E_2 = 1 - \boldsymbol{P}^*\left[D^*_{cp}\left\{\theta - g\boldsymbol{P}^*\right\}\right]v/H,$$

$$E_3 = -\lambda^*_{cp}v\boldsymbol{P}^*/H, \quad E_4 = -D^*_{Tp}v\boldsymbol{P}^*/H,$$

where

$$g = \lambda^*_{Tp}D^*_{cp} - \lambda^*_{cp}D^*_{Tp}.$$

The nondimensional material properties appearing in Eq. (45) can be rewritten using the basic property ratios of the particles and the fluid, Eq. (46), i.e.,

$$\lambda^*_{Tp} = \left(\sigma'_{TT} - \kappa_T\kappa_c\sigma'_{Tc}\right)/(1 - \kappa_T\kappa_c),$$

$$\lambda^*_{cp} = \kappa_T\left(\sigma'_{cT} - \sigma'_{cc}\right)/(1 - \kappa_T\kappa_c),$$

$$D^*_{Tp} = \kappa_c\left(\sigma'_{Tc} - \sigma'_{TT}\right)/(1 - \kappa_T\kappa_c),$$

$$D^*_{cp} = \left(\sigma'_{cc} - \kappa_T\kappa_c\sigma'_{cT}\right)/(1 - \kappa_T\kappa_c).$$

These material functions vary across the barrier and, when they are known, it is possible to solve the set of Eqs. (36) and (37) for the unknown solute flux $\{\boldsymbol{j}\}$. Due to the assumption of steady state heat conduction and mass diffusion, the heat flux and the solute flux are constant. This conclusion allows one to obtain a solution in a simple manner. The set of Eqs. (36) and (37) has been solved for gradients of the macroscopic temperature and concentration and, subsequently, integrated utilizing the boundary conditions at the barrier faces, i.e., known temperatures $\{T\}_1$, $\{T\}_2$ ($\{T\}_1 > \{T\}_2$) and known solute concentrations $\{c\}_1$, $\{c\}_2$, with $\{c\}_1 = \{c\}_2$. The resulting expression for the dimensionless mass flux of the diffusing solute, when the flow is driven by temperature difference ($\{T\}_1 - \{T\}_2$), assumes the following form

$$\{j\}/j_f = \frac{A_2(\Delta 2R)}{\kappa_c(A_1A_4 - A_2A_3)}$$

where symbol j_f stands for the solute flux in the fluid when the particles are absent and

$$A_1 = \int_0^{(\Delta/\ell)} \lambda^{ef}_{T\perp}(z^*)/\left[\lambda_{Tf}g_{ef}(z^*)\right]\,dz^*,$$

$$A_2 = \int_0^{(\Delta/\ell)} D^{ef}_{T\perp}(z^*)/\left[D_{cf}g_{ef}(z^*)\right]\,dz^*,$$

$$A_3 = \int_0^{(\Delta/\ell)} \lambda^{ef}_{c\perp}(z^*)/\left[\lambda_{Tf}g_{ef}(z^*)\right]\,dz^*,$$

$$A_4 = \int_0^{(\Delta/\ell)} D^{ef}_{c\perp}(z^*)/\left[D_{cf}g_{ef}(z^*)\right]\,dz^*,$$

where

$$g_{ef} = \left(\lambda^*_{Tp}D^*_{cp} - \lambda^*_{cp}D^*_{Tp}\right)/(\lambda_{Tf}D_{ef}), \quad z^* = z/\ell$$

and $\ell = 2R$ for the disk-like particles and $\ell = L$ for the rod-like particles.

Calculations of the dimensionless solute flux follow essentially the same procedure as in the case of pure mass diffusion. Nevertheless, this time $\{j\}/j_f$ depends not only on the structural parameters (v and ε), shape of the particles, and geometrical parameter ($\Delta/(2R)$), but also on five dimensionless ratios of particle/fluid properties, i.e., σ_{TT}, σ_{Tc}, σ_{cT}, σ_{cc}, m and on two dimensionless parameters characterizing the role of the coupled phenomena, i.e., κ_T and κ_c. Results of calculations for parameter values that give the highest effectiveness of the barrier as far as control of the solute flow is concerned are presented in Figs. 5–10.

The main factor affecting the solute flux is the class of shapes of the particles. Two classes of shapes, i.e., the disk-like and the rod-like particles, were studied. Results displayed in Figs. 5–10 show that the former class is significantly more effective.

The diffusion-thermo effect (Dufour) coefficient λ_c and the thermo-diffusion effect (Soret) coefficient D_T may be either positive or negative and are usually much smaller than the thermal conductivity λ_T and the solute diffusivity D_c [19]. The Onsager reciprocal relations of thermodynamics of irreversible processes give information as to the interrelation of the two coupled (cross) effects, the Defour and the Soret. According to these relations the thermodynamic coefficients of the diffusion-thermo and the thermo-diffusion are equal to each other. The corresponding experimental transport coefficients in general are not the phenomenological, thermodynamic coefficients and the experimental cross coefficients do not necessarily have to obey the Onsager relations [22]. Nevertheless, the relation $\lambda_T D_c - \lambda_c D_T > \phi$ is valid.

Thermal conductivity λ_{Ts} of the solid particles may be smaller or greater than thermal conductivity λ_{Tf} of the fluid. The Dufour λ_{cs} and the Soret D_{Ts} coefficients in the solid particles are, however, much smaller than the corresponding coefficients λ_{Tf} and D_{cf} in the carrier fluid. Also the solute diffusivity D_{cs} is smaller in the

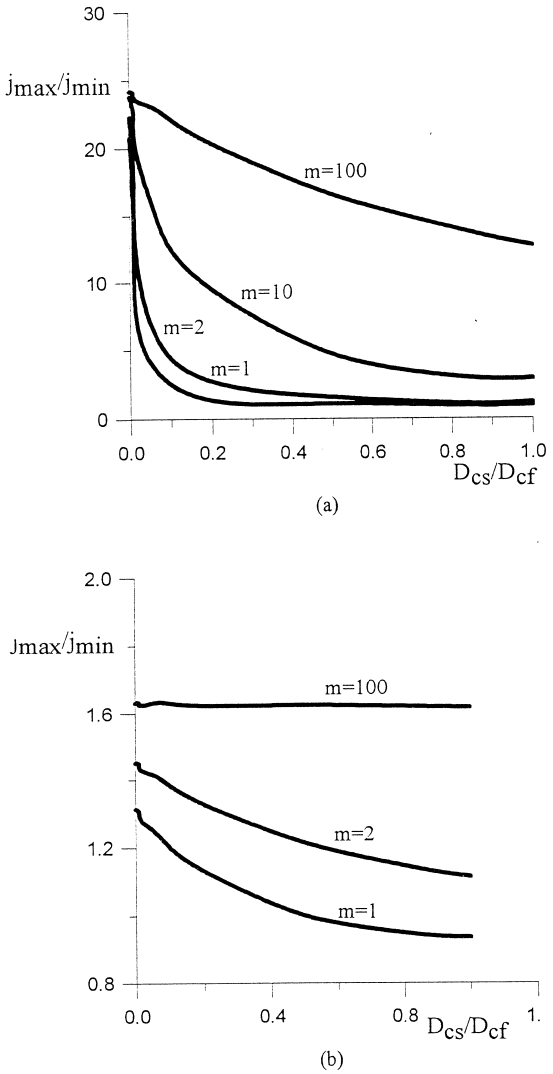

Fig. 5. Variation of the barrier effectiveness j_{max}/j_{min} as a function of the particle/fluid diffusivity ratio $D_{cs}/D_{cf} = \sigma_{cc}$ and solubility m for $\sigma_{TT} = 10^3$, $\kappa_T = \kappa_c = 10^{-3}$, $\tilde{\nu} = 0.3$, $\varepsilon(\varepsilon^*) = 100$: (a) in the case of disk-like particles $\Delta/(2R) = 10$; (b) in the case of rod-like particles $\Delta/L = 10$.

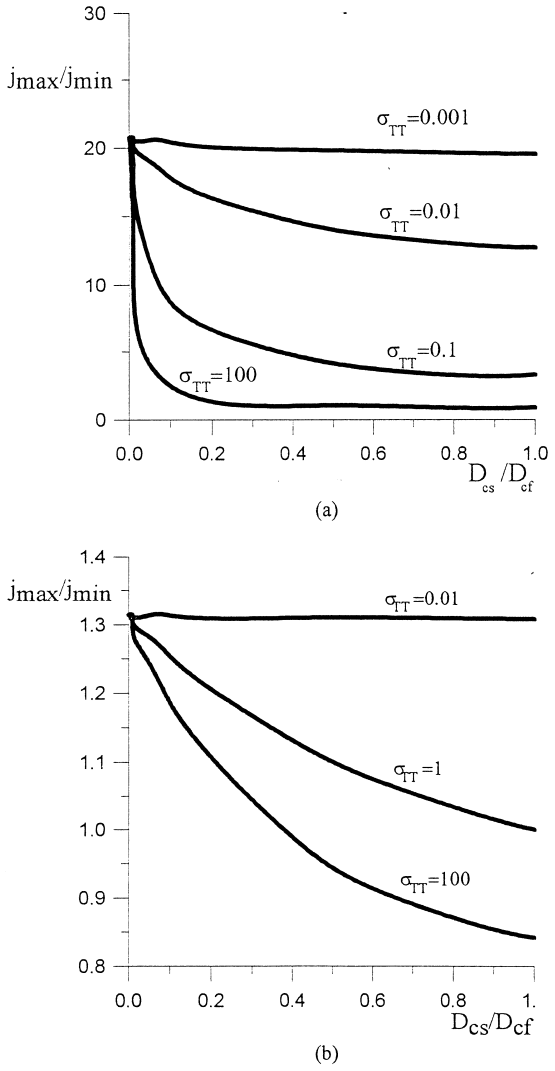

Fig. 6. Variation of the barrier effectiveness j_{max}/j_{min} as a function of the particle/fluid diffusivity ratio $D_{cs}/D_{cf} = \sigma_{cc}$ and the particle/fluid thermal conductivity ratio $\sigma_{TT} = \lambda_{Ts}/\lambda_{Tf}$ for $m = 1$, $\kappa_T = \kappa_c = 10^{-3}$, $\tilde{\nu} = 0.3$, $\varepsilon(\varepsilon^*) = 100$: (a) in the case of disk-like particles $\Delta/(2R) = 10$; (b) in the case of rod-like particles $\Delta/L = 10$.

particles than the solute diffusivity D_{cf} in the fluid while the inverse relation holds for the solubility of the solute in the particles and in the fluid. Thus, in the calculations we have assumed that σ_{Tc} and σ_{cT} are both equal to zero.

We have found that, in the case considered here, the influence of the dimensionless Dufour κ_T and Soret κ_c coefficients of the fluid on the barrier effectiveness j_{max}/j_{min} is practically negligible. The barrier effectiveness is, however, very sensitive to variation in the particle/fluid diffusivity σ_{cc}, thermal conductivity σ_{TT} and the solute solubility m ratios. It decreases with an increase of σ_{cc} and σ_{TT} (Fig. 5). The barrier is most effective for $\sigma_{cc} = D_{cs}/D_{cf} = 0$. An increase in the solute solubility also causes an increase in j_{max}/j_{min} but does not exceed the corresponding values for $\sigma_{cc} = 0$ (Fig. 6).

For the rod-like particles and certain values of parameters σ_{cc}, σ_{TT} and m, the effectiveness of the barrier attains values smaller than unity (Fig. 5b and 6b). This result suggests that for $j_{max}/j_{min} < 1$, it is necessary to rotate axes of the rod-like particles from being perpen-

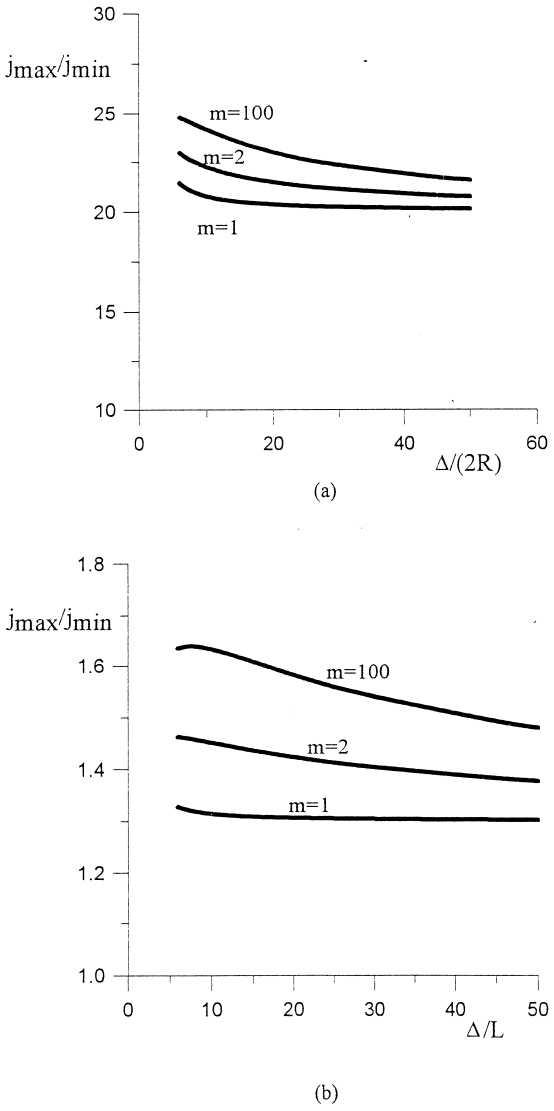

Fig. 7. Variation of the barrier effectiveness j_{max}/j_{min} as a function of nondimensional thickness of the barrier and solubility m for $\sigma_{TT} = 10^3$, $\sigma_{cc} = 0$, $\kappa_T = \kappa_c = 10^{-3}$, $\varepsilon(\varepsilon^*) = 100$, $\tilde{v} = 0.3$: (a) in the case of disk-like particles (nondimensional thickness is defined as $\Delta/2R$); (b) in the case of rod-like particles (nondimensional thickness is defined as Δ/L).

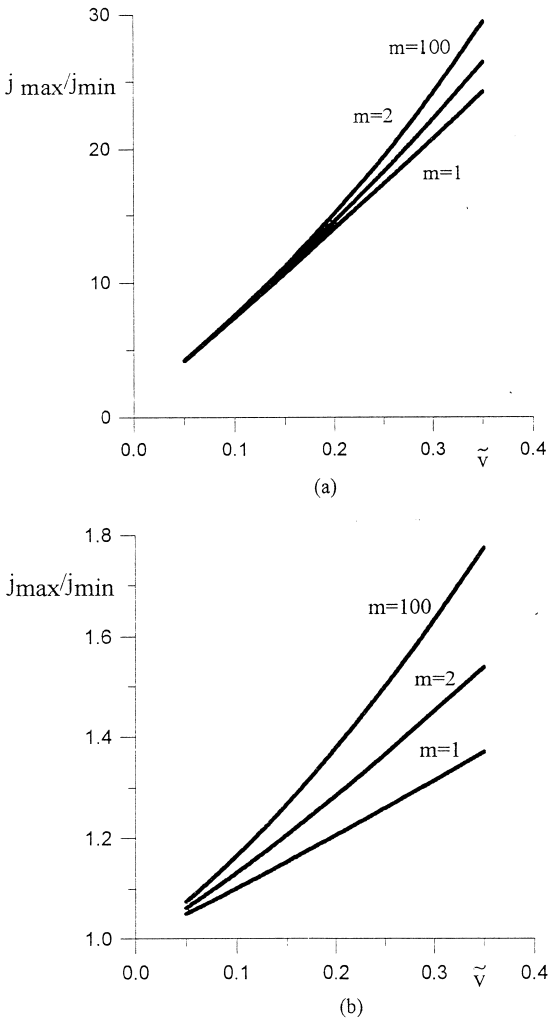

Fig. 8. Variation of the barrier effectiveness j_{max}/j_{min} as a function of the particle volume fraction and solubility m for $\sigma_{TT} = 10^3$, $\sigma_{cc} = 0$, $\kappa_T = \kappa_c = 10^{-3}$, $\varepsilon(\varepsilon^*) = 100$: (a) in the case of disk-like particles $\Delta/(2R) = 10$; (b) in the case of rod-like particles $\Delta/L = 10$.

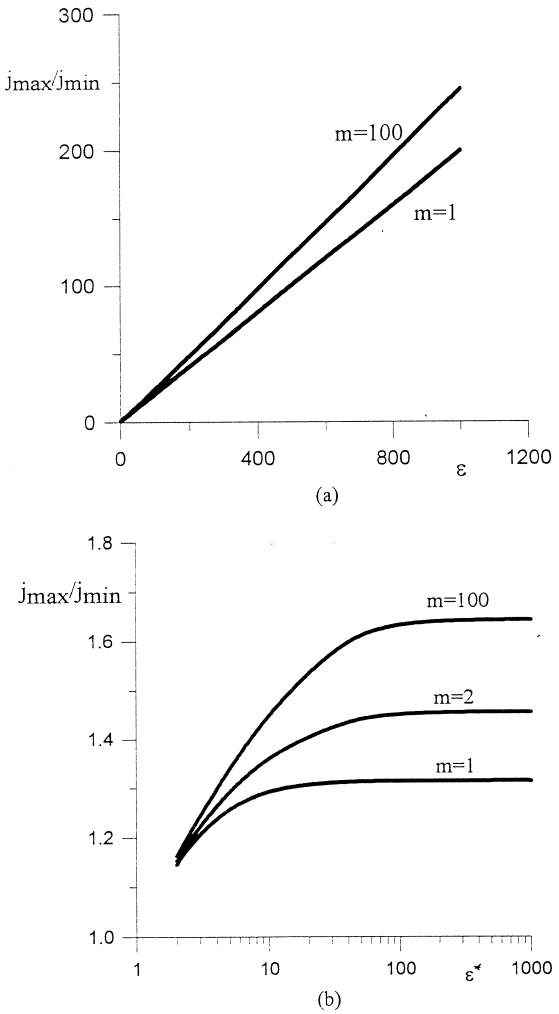

Fig. 9. Variation of the barrier effectiveness j_{max}/j_{min} as a function of the particle aspect ratio $\varepsilon(\varepsilon^*)$ and solubility m for $\sigma_{TT} = 10^3$, $\sigma_{cc} = 0$, $\kappa_T = \kappa_c = 10^{-3}$, $\tilde{v} = 0.3$: (a) in the case of disk-like particles $\Delta/(2R) = 10$; (b) in the case of rod-like particles $\Delta/L = 10$.

dicular to being parallel to the barrier faces in order to increase the solute flux.

The ratio of the barrier thickness Δ to the main particle dimension ($2R$ for the disk-like particles and L for the rod-like particles), although not significant in absolute terms, has a greater influence on the barrier effectiveness than in the pure diffusive case (Fig. 7). An increase in the solute solubility m leads to an increase in j_{max}/j_{min}.

The mean volume fraction $\tilde{v}$ of the particles is a significant factor in controlling solute flow (Fig. 8). The greater the value of the mean volume fraction $\tilde{v}$ of the particles, the broader the range of control of the solute flow. An increase in solubility m of the solute leads to an increase in the barrier effectiveness. This effect is greater for the rod-like particles than for the disk-like particles.

Particle aspect ratio appears to be one of the most important factors in controlling the solute flow (Fig. 9). An increase of ε in the case of the disk-like particles (ε^* in the case of the rod-like particles) leads to a broadening of the range in which the solute flux may be controlled by the particle rotation. An increase in the solute solubility again affects the barrier effective-

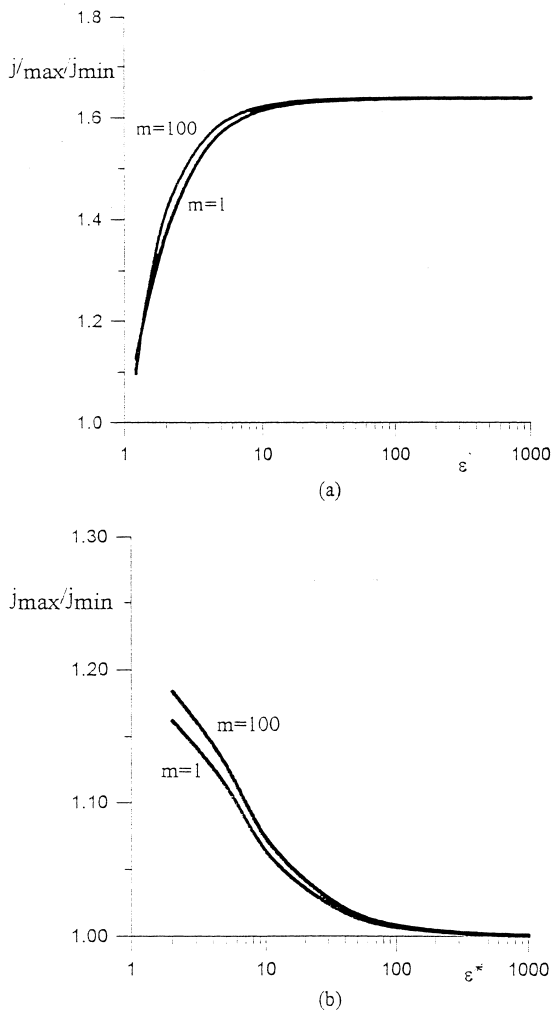

Fig. 10. Variation of the barrier effectiveness j_{max}/j_{min} as a function of the particle aspect ratio $\varepsilon(\varepsilon^*)$ and solubility m for $\sigma_{TT} = 10^3$, $\sigma_{cc} = 0$, $\kappa_T = \kappa_c = 10^{-3}$ and $\tilde{v}$ limited by the requirement that the particles have enough free space to permit their rotation (the relation between $\tilde{v}$ and $\varepsilon(\varepsilon^*)$ is similar to the one utilized in Fig. 4b): (a) in the case of disk-like particles $\Delta/(2R) = 10$; (b) in the case of rod-like particles $\Delta/L = 10$.

ness more for the rod-like particles than for the disk-like particles.

For higher volume fraction of the particles, the requirement of availability of sufficient space to permit rotation of the particles leads to limitations on the maximum permissible volume fraction $\tilde{v}$. For the disk-like particles, this limit is identical with the one given in the previous section, while for the rod-like particles it can be written as $\tilde{v}_{\max} \leq 2/(3\varepsilon^*)$. If these limitations are taken into account, the barrier effectiveness is significantly reduced (Fig. 10).

6. Conclusions

The effective medium theory has been derived for the coupled phenomena of heat conduction and mass diffusion of the solute in a heterogeneous medium made of two constituents. Ideal thermal contact and diffusive conditions at the interfaces of the constituents were assumed but different solubilities of the solute in each constituent was permitted. It has been found that the relations between the macroscopic heat and solute fluxes and the macroscopic temperature and concentration in the medium were generally nonlocal and that they reduce to the local form only for slowly varying macroscopic temperature and concentration fields. In this particular case, the relations assume the forms that are identical to those valid inside each constituent. The effective material functions, which appear in the macroscopic relations between the heat and mass fluxes and the temperature and concentration gradients, are dependent on the bulk dimension of the medium. Only at a certain distance away from the boundary, with this distance being of the order of the greatest microdimension, they may be treated as the effective properties of the heterogeneous medium. These effective properties depend on the details of the microstructure of the heterogeneous medium and on the all thermal and diffusive properties of the constituents.

The theory has been applied to the problem of control of solute flow using a smart barrier. The barrier is made of suspension of spheroidal particles randomly distributed in a carrier fluid resulting in variation of its thermal and diffusive properties. A change of the effective material properties is achieved by externally induced change in the orientation of the particles. The analysis has been limited to the cases of solute flux being driven by: (i) concentration difference with coupled phenomena neglected, and (ii) temperature difference. Results of the analysis indicate that the barrier may be effective in controlling the mass flow of the diffusing species provided that a proper combination of the particles (with proper shape, size and properties) and carrier fluid are chosen. Two classes of particle shapes were studied, i.e., rod-like particles and disk-like particles. The results show that the latter one provides a much wider range of control of the solute flux, i.e., higher barrier effectiveness, for both cases of the concentration difference and temperature difference driven flows. The barrier effectiveness also increases for higher volume fraction of the particles, higher aspect ratio of the particles and smaller thickness of the barrier (as compared to the major particle dimension). Greater value of solubility of the solute in the fluid than in the solid particles, smaller ratios of particle/fluid diffusivity and particle/fluid thermal conductivity also contribute to an increase of the effectiveness of the barrier.

Acknowledgements

The authors would like to acknowledge support for this work received from the State Committee for Scientific Research (KBN) of Poland and from NSERC of Canada.

Appendix A

For equilibrium distribution of concentration in the heterogeneous medium, i.e., for

$$T = \{T\} = \text{const}, \quad \{c\} = \text{const}. \tag{A1}$$

the distribution of the concentration of the diffusing species can be expressed as

$$c(\boldsymbol{x}) = P_{\text{eq}}(\boldsymbol{x})\{c\}. \tag{A2}$$

When Eq. (A2) is substituted into Eq. (15), the latter equation reduces to

$$M(\boldsymbol{x}, \Omega)P_{\text{eq}}(\boldsymbol{x}, \Omega) = \left\{M(\boldsymbol{x})P_{\text{eq}}(\boldsymbol{x})\right\} = \text{const}. \tag{A3}$$

Noting, from Eq. (A2), that the following relation holds

$$\left\{P_{\text{eq}}(\boldsymbol{x})\right\} = 1,$$

the equilibrium distribution function can be written as

$$P_{\text{eq}}(\boldsymbol{x}) = \frac{1}{\left[m(1-v)+v\right]}\theta(\boldsymbol{x}) + \frac{m}{\left[m(1-v)+v\right]}\left[1-\theta(\boldsymbol{x})\right]. \tag{A4}$$

When the equilibrium conditions in the medium are not met, the concentration can be expressed as

$$c(\boldsymbol{x}) = P_{\text{eq}}(\boldsymbol{x})\{c\} + c'(\boldsymbol{x}) \tag{A5}$$

where the last term stands for the fluctuation of the concentration. Substituting the above expression into

the left-hand side of Eq. (15), simplifying the result using the following property

$$\{Mc'\} \ll \{c\}$$

and carrying out the ensemble averaging of the resulting equation, one obtains the following relation

$$\{Mc\} = MP_{eq}\{c\}. \tag{A6}$$

References

[1] Z.P. Shulman, Utilization of electric and magnetic fields for control of heat and mass transfer in dispersed systems (suspensions), Heat Transfer — Soviet Research 14 (1982) 1–23.

[2] C. Zhang, J.R. Lloyd, Control of radiation heat transfer through a composite window featuring ER fluid: a conceptual investigation, J. Engng. Physics and Thermophysics 66 (1994) 115–125.

[3] P. Furmanski, J.M. Floryan, A thermal barrier with adaptive heat transfer characteristics, Transactions of the ASME, J. Heat Transfer 116 (1994) 302–310.

[4] P. Furmanski, J.M. Floryan, Heat conduction through a barrier made of a suspension of dislike particles, Transactions of the ASME, J. Heat Transfer 117 (1995) 755–757.

[5] R. Caps, J. Hetfleisch, J. Fricke, Switchable thermal insulation for solar heating, in: Proceedings of 24th International Thermal Conductivity Conference, October 26–29, Pittsburgh, PA, 1997.

[6] J. Bear, J.M. Buchlin, Modeling and Applications of Transport Phenomena in Porous Media, Kluwer, Dordrecht, 1991.

[7] R.G. Carbonell, S. Whitaker, Heat and mass transfer in porous media, in: J. Bear, M.Y. Corapciooglu (Eds.), Fundamentals of transport phenomena in porous media, Martinus Nijhoff Publishers, Dortrecht/Boston/Lancaster, 1984, pp. 121–198.

[8] P. Furmanski, Effective macroscopic description for heat conduction in heterogeneous media, Int. J. Heat Mass Transfer 37 (1994) 2993–3002.

[9] P. Furmanski, J.M. Floryan, Wall effects in heat conduction through a heterogeneous material, Int. J. Heat Mass Transfer 37 (1994) 1945–1955.

[10] S. Torquato, Random heterogeneous media: microstructure and improved bounds on effective properties, Appl. Mech. Rev. 44 (1991) 37–76.

[11] W. Strieder, R. Aris, Variational Methods Applied to Problems of Diffusion and Reaction, Springer-Verlag, NewYork/Heidelberg/Berlin, 1973.

[12] D. Ryan, R.G. Carbonell, S. Whitaker, Effective diffusivities for catalyst pellets under reactive conditions, Chem. Engng. Sci. 35 (1980) 10–16.

[13] J. Bear, Y. Bachmat, Advective and diffusive fluxes in porous media, in: J. Bear, M.Y. Corapciooglu (Eds.), Advances in Transport Phenomena in Porous Media, Martinus Nijhoff Publishers, Dortrecht/Boston/Lancaster, 1987, pp. 21–46.

[14] Yu.A. Buyevich, On the fluctuations of concentration in disperse systems. Spectral description of the random concentration field and application to solute dispersion in packed beds, Chem. Engng. Sci. 27 (1972) 1699–1708.

[15] D.L. Koch, J.F. Brady, The symmetry properties of the effective diffusivity tensor in anisotropic porous media, Phys. Fluids 30 (1987) 642–650.

[16] D.L. Koch, J.F. Brady, Dispersion in fixed beds, J. Fluid Mechanics 154 (1985) 399–427.

[17] D.L. Koch, J.F. Brady, A non-local description of advective-diffusion with application to dispersion in porous media, J. Fluid Mechanics 180 (1987) 387–403.

[18] Y. Bachmat, J. Bear, Transport phenomena in porous media — basic equations, in: J. Bear, M.Y. Corapciooglu (Eds.), Fundamentals of Transport Phenomena in Porous Media, Martinus Nijhoff Publishers, Dortrecht/Boston/Lancaster, 1984, pp. 3–62.

[19] R.B. Bird, W.E. Stewart, W.N. Lightfoot, Transport Phenomena, Wiley, New York, 1960.

[20] P. Furmanski, Heat conduction in composites: homogenization and macroscopic behavior, Appl. Mech. Rev. 50 (1997) 327–356.

[21] S. Yamashita, H. Hatta, K. Sugano, K. Murayama, Fiber orientation control of short fiber composites. Experiment, J. Composite Materials 23 (1989) 32–41.

[22] H.J.M. Hanley (Ed.), Transport Phenomena in Fluids, Marcell Dekker, New York, 1969.